Sedimentary Geology 448 (2023) 106367

Contents lists available at ScienceDirect

Sedimentary Geology

journal homepage: www.elsevier.com/locate/sedgeo

Paleogene evolution of the External Rif Zone (Morocco) and comparison with other western Tethyan margins

Manuel Martín-Martín [a,*], Francesco Guerrera [b], Juan Carlos Cañaveras [a], Francisco Javier Alcalá [c,d], Francisco Serrano [e], Alí Maaté [f], Rachid Hlila [f], Soufian Maaté [g], Mario Tramontana [b], Antonio Sánchez-Navas [h], Eline Le Breton [i]

[a] Departamento de Ciencias de la Tierra y Medio Ambiente, University of Alicante, AP 99, 03080 Alicante, Spain
[b] Dipartimento di Scienze Pure e Applicate (DiSPeA), Università degli Studi di Urbino Carlo Bo, Campus Scientifico E. Mattei, 61029 Urbino, Italy
[c] Departamento de Desertificación y Geo-Ecología, Estación Experimental de Zonas Áridas (EEZA–CSIC), 04120 Almería, Spain
[d] Instituto de Ciencias Químicas Aplicadas, Facultad de Ingeniería, Universidad Autónoma de Chile, 7500138 Santiago, Chile
[e] Departamento de Ecología y Geología, University of Málaga, 28071 Málaga, Spain
[f] Laboratoire de Géologie de l'Environnement et Ressources Naturelles, FS, Université Abdelmalek Essaâdi, B.P. 2121, Mhannech II, 93002 Tetouan, Morocco
[g] Laboratoire de Géologie Appliquée, Facultédes Sciences et Techniques, Université Moulay Ismaïl, B.P. 509, Boutalamine, 52000 Errachidia, Morocco
[h] Departamento de Mineralogía y Petrografía, University of Granada, 18071 Granada, Spain
[i] Department of Earth Sciences, Institute for Geological Sciences, Freie Universität Berlin, Berlin, Germany

ARTICLE INFO

Article history:
Received 21 December 2022
Received in revised form 6 March 2023
Accepted 7 March 2023
Available online 16 March 2023

Editor: Dr. Massimo Moretti

Keywords:
Foreland basin system
Tectono-sedimentary evolution
Paleogene
Western External Rif
Northwestern African margin
Western Tethys margins

ABSTRACT

The Paleogene evolution of the NW margin of the African Plate (Western External Rif Zone) was studied by means of multidisciplinary analyses of twenty-one stratigraphic logs, including tectofacies recognition, petro-mineralogical results, and thicknesses analysis. Four stratigraphic intervals were recognized separated by three unconformities coarsely aligned with the Cretaceous–Paleogene, Eocene–Oligocene and Oligocene–Miocene boundaries, respectively. Tectofacies appear from the late Ypresian being more frequents from the Oligocene as the tectonic activity increases. The petrology of detrital suites indicates recycled orogen-derived sediments, with quartz supplied from metamorphic rocks of the Atlas orogen and/or the African craton. On the basis of Mesozoic clay mineral assemblages reported in the literature, the clay mineralogy of mudstones suggests upper Jurassic to upper Cretaceous terrains from the Internal Intrarif as the main source area of the Paleocene–Eocene successions, with sediment provenance reversion during the Oligocene and additional contribution of Paleocene to lower Eocene suites. The different displacement capability of the identified aluminic-magnesic clay mineralogy enabled to deduce the relative proximity of the source area. These findings point out a complex sedimentary evolution characterized by a mixture of different lithotypes dating back to upper Jurassic. X-ray parameters helped to identify evidences of synsedimentary tectonics overprinting the inherited mineralogy during some periods with weak burial diagenesis at most. During the Paleogene a foreland basin is formed mainly in the Mesorif and Prerif sub-domains. This foredeep was represented by two 'sub-geosynclines' separated by a relative bulge located in the External Mesorif. The Internal Intrarif could represent the relative orogenic front, advancing on the External Intrarif. The Eocene forebulge was located in the Ridges Domain, while the Gharb Basin was the backbulge of the system. During the Oligocene the depocentral area migrated southward and a homogeneization of thicknesses took also place in the whole margin. In this new configuration, the foredeep would be located in the External Mesorif (previously a relative bulge) while the Ridges Domain and the Gharb Basin continued to act as the system forebulge and backbulge, respectively. A comparison with the Paleogene evolution of other western Tethys external margins (Betic Chain, Tunisian Tell, Sicilian Maghrebids, and Apennines) has revealed more similarities than differences. The effects of the Eo-Alpine tectonics are recognized everywhere even if they decrease both from N to S, and from W to E in the different considered margins. The evolution of the compared margins shows a common pre-foredeed (Paleocene-Eocene) and beginning of foredeep (Oligocene) stages in the foreland basins.

1. Introduction

The Alpine Rif Chain (W Maghrebian Chain), is located in the NW margin of the African Plate (Fig. 1A) and is linked to the alpine evolution

* Corresponding author at: Departamento de Ciencias de la Tierra y del Medio Ambiente, Universidad de Alicante, Campus San Vicente, San Vicente del Raspeig, 03080 Alicante, Spain.
E-mail address: manuel.martin@ua.es (M. Martín-Martín).

https://doi.org/10.1016/j.sedgeo.2023.106367

of the westernmost Tethys and the subsequent opening of the Mediterranean Sea (Doglioni, 1992; Guerrera et al., 1993, 2005; Doglioni et al., 1999; Chalouan et al., 2008; Guerrera and Martín-Martín, 2014; Critelli et al., 2017; Müller et al., 2018). This Chain has classically been divided (Chalouan et al., 2008; among others) into (i) the Internal Zone, which derived from the Mesomediterranean Microplate (Guerrera et al., 2021); (ii) the Flysch Zone, which is characterized by units resulting from the Maghrebian Flysch Basin (Guerrera et al., 1993, 2005, 2021); and (iii) the wide External Zone, which represents the deformed African NW margin (Martín-Martín et al., 2022a). This last consists of Mesozoic to Miocene successions detached from their Paleozoic substratum (Atlas and Mesetas), and records the effects of the Miocene–Quaternary deformation related to the orogenic evolution of the Maghrebian Chain.

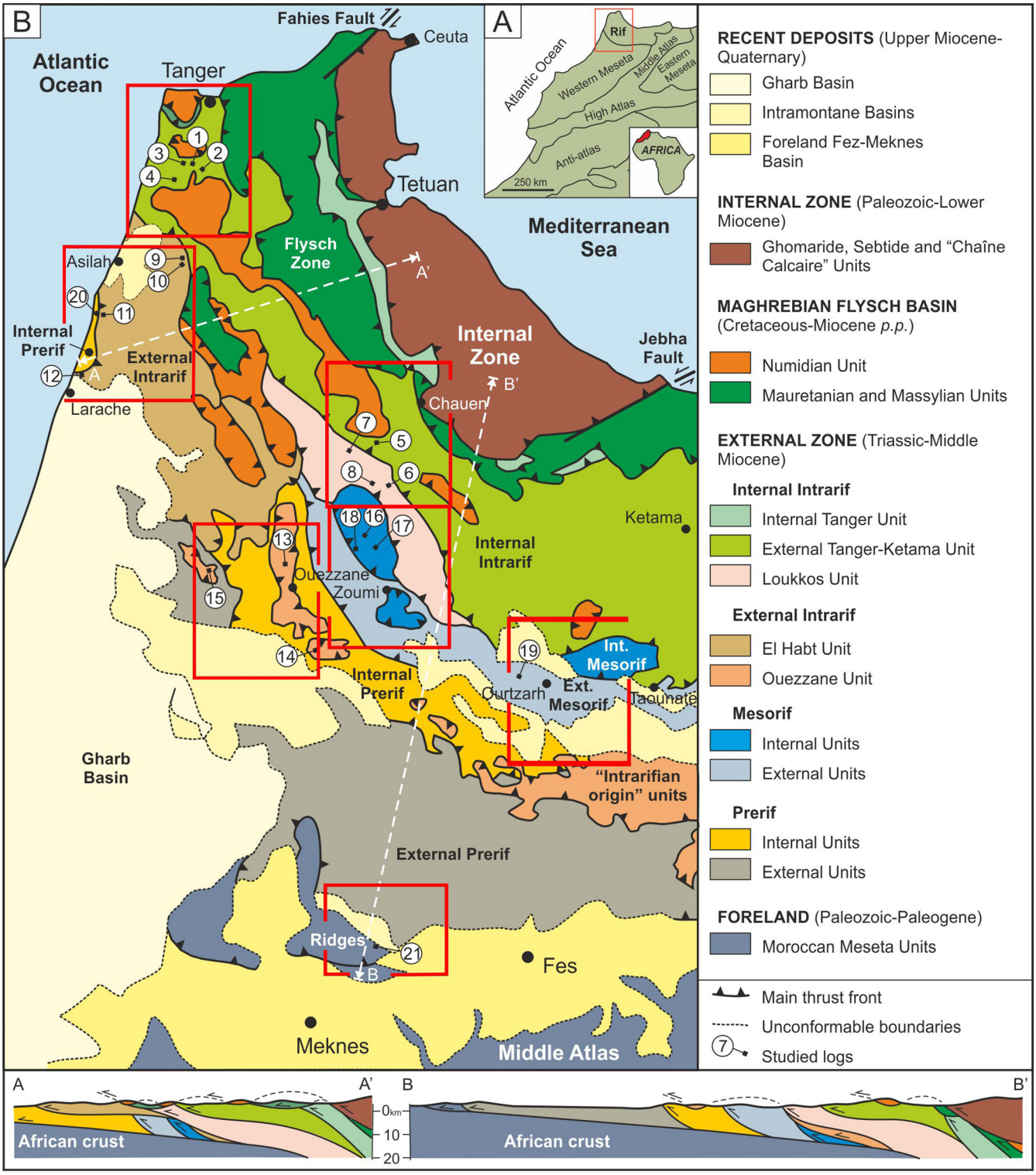

Fig. 1. Geological map of the Rif Chain. (A) geological sketch map of NW Africa; (B) geological map of the Rif Chain showing the studied seven sectors and the location of the measured and reconstructed twenty-one stratigraphic successions (Logs). The whole structural data are in the Supplemenatry Material A1.

The External Rif Zone (Fig. 1B) represents a portion of the northern African continental crust and the passive paleo-margin of the more internal Maghrebian Basin (de Frizon Lamotte et al., 2017). This margin experienced a progressive Cenozoic deformation in a foreland basin evolutionary context (Abbassi et al., 2021), where the Gharb Basin acted as a part of the foreland basin during Late Miocene and the Atlas-Mesetas system as the relative foreland (Chalouan et al., 2008).

Based on age and structural position, Suter (1980a, 1980b) subdivided the External Rif Zone (from internal to external areas) into the following subdomains: Intrarif (mainly Cretaceous deposits), Mesorif (mainly Jurassic carbonate deposits to deep water turbidites), and Prerif (Cenozoic olistostromes). The latter are characterized by fragments of ultrabasic rocks from an oceanic basement, Jurassic carbonate platform deposits, and Triassic basic subvolcanic rocks in a Miocene marly matrix (Fig. 1B). For the western Rif, Suter (1980a) proposed a further division: (i) the Intrarifian Zone consisting of the Internal Tanger, External Ketama-Tanger, and Loukkos units; and (ii) the allochthonous units of 'Intrarifian origin' forming the El Habt and Ouezzane nappes. These nappes consist of Cretaceous–Cenozoic successions with Intrarifian affinity (described in detail in this paper), and overthrusting the Mesorif and Prerif subdomains. These units were recently renamed as the Internal and External Intrarif, respectively (Martín-Martín et al., 2022a). Moreover, the External Rif Zone has been divided into the western and eastern Rif Zones regarding the city of Ketama (Chalouan et al., 2008). The western External Rif Zone consists of sedimentary successions, while some of the eastern units show a slight metamorphism.

At the end of Mesozoic, the African Plate was in a southern position and separated from the Mesomediterranean Microplate by means of the Maghrebian Flysch Basin, which was one of the western branches of the westernmost Tethys Ocean. The closure of the western Maghrebian Flysch Basin (Guerrera et al., 1993, 2021; Chalouan et al., 2008; Guerrera and Martín-Martín, 2014; Müller et al., 2018) would have started from the latest Cretaceous (Stampfli and Kozur, 2006) but mostly happened during the latest Oligocene *p.p.*–Miocene *p.p.* with the extrusion of the Maghrebian Flysch Basin units and the propagation of the deformation in the External Rif Zone.

Although previous models already proposed the occurrence of a southern oceanic branch of the Tethys, the confirmation of Jurassic ophiolite-type basic rocks related to an oceanic crust at the base of the Maghrebian Flysch Basin is relatively recent (Durand Delga et al., 2000; Boukaoud et al., 2021). The External Rif Zone and Maghrebian Flysch Basin would have behaved as a complex foreland basin system during a large part of Cenozoic, due to subduction beneath the Mesomediterranean Microplate (Guerrera et al., 2005; Abbassi et al., 2021). The roll-back of the subducting oceanic crust of the Maghrebian Flysch Basin would lead to the opening of the Mediterranean Sea as a back-arc basin from late Oligocene. Benzaggag (2016) pointed out the presence of another possible oceanic suture between the Intrarif and the Mesorif (eastern External Rif Zone) by the occurrence of basalts, breccias, and serpentinites. Contrarily, Michard et al. (2014, 2018) proposed that the Mesorif suture zone corresponds to the trace of the displacement of the west African Atlantic margin surrounding the northwestern Morocco Meseta. Considering both one and the other hypothesis for this Intrarif-Mesorif suture, the aforementioned foreland basin would be more complex, and the paleogeography of the western Tethys should be changed considering the presence of more oceanic branches than those already proposed.

Although the compression of the Tethyan domains started with the latest Cretaceous tectonic inversion (Stampfli and Kozur, 2006) and an important folding should have occurred during the Paleogene, the main compressional deformation proposed for the External Rif Zone developed during the Miocene (Zakir et al., 2004; Chalouan et al., 2006). A nappe structuring consisting of units detached from their original paleogeographic position and overriding the more external units took place during this last period (Chalouan et al., 2008; Vázquez et al., 2013; Jabaloy-Sánchez et al., 2015). Therefore, the original stratigraphic successions have completely been deformed and tectonically translated outwards, and therefore the new paleogeographic and paleotectonic reconstructions must consider these factors. Also strike-slip tectonics overprinted on this deformation during the Miocene (Azdimousa et al., 2007). According to AitBrahim et al. (2002), these tectonics would be accomplished in the Rif by a main compressional axis rotating from *E*-W to approximately N-S during the Paleogene to present time span.

Despite the recent studies focused on the External Rif Zone (Maaté et al., 2017, 2018; Martín-Martín et al., 2022a, 2022b), many issues remain open. There are related to (i) the lack of comparable data derived from the many local studies with different objectives carried out; (ii) the use of different, unrelated terminologies for each single studied sector; (iii) the intrinsic difficulty to interpret the pre-deformation paleogeographic location of unrooted tectonic units and (iv) the lack of a broad and multidisciplinary study for the whole External Rif Zone. Conversely, a growing consensus there is about the tectonic setting of the External Rif Zone (de Frizon Lamotte et al., 2017), and about the interpretation considering the Intrarif units as upper Jurassic to Miocene sedimentary successions deposited in a deep basin located on oceanic and/or thinned continental crust, and probably in connection with the Maghrebian Basin (Michard et al., 2007).

In this context, this paper presents a detailed study of the whole western External Rif Zone with special focus on the relationships between tectonics and sedimentation in general, the subsidence analysis and synsedimentary tectonic activity in particular. The new data obtained on the upper Cretaceous-Paleogene successions allow considering the western Intrarif as a complex foreland basin, thus improving the western External Rif Zone characterization and highlighting the presence of paleogeographic and paleotectonic events in the area. A comparison with the Paleogene evolution of other central-western Mediterranean margins of the same chains-system is included in order to obtain constrains at the Western Tethys framework.

2. Methods

The used methodology includes: (1) Field analyses, including stratigraphic reconstruction (logging) of representative successions, sampling, and structural observations. The lithofacies were unified as homogeneous stratigraphic intervals based on lithological features, sedimentary structures, sedimentary continuity and presence of unconformities, stacking patterns, marker-beds, and migration of depositional systems. (2) Laboratory analyses, including biostratigraphy and chronostratigraphy, petrography of detrital suites, and mineralogy of mud and clay suites. (3) Data processing, including analysis of results to perform paleogeographic and paleotectonic. (4) Interpretation of geological and tectonic events, and correlation at regional scale. This multidisciplinary approach enabled reconstructing the depositional systems and related paleoenvironments, and subdividing the stratigraphic record into sedimentary depositional sequences attending to lithostratigraphic characters, biostratigraphic analyses and observed unconformities.

Biostratigraphic and chronostratigraphic analyses have been carried out on 198 samples by planktonic foraminifera assemblages (Fig. 2). Samples were subjected to conventional washing and splitting by sieves of 150 μm (the main studied fraction) and 125 μm. Fraction 125–150 μm was observed, in order to verify the potential existence of small species of genera such as *Parvuloglobigerina*, *Guembelitria* or *Globoconusa*, and also species as *G. angulisuturalis* or *G. kugleri*. Reworked organic components were considered part of the detrital fraction to recognize the useful oldest age. Four samples referable to Oligocene deposits were analyzed by using calcareous nannoplankton, due to the rarity of planktonic foraminifera. Biozonations of Berggren et al. (1995), Berggren and Pearson (2005, 2006) and subsequent revision of Wade et al. (2011), as well as the Global Standard Chronostratigraphic Scale (Lourens et al.,

2004) were considered for biostratigraphic constraints and chronostratigraphic correspondence. For Miocene deposits, the standard biozonation by Blow (1969) in combination with the more significant planktonic foraminiferal bio-events checked in the Mediterranean area were also considered (Serrano, 1992; Di Stefano et al., 2008). The standard zonation of Martini (1971) was used for biostratigraphy of calcareous nannoplankton.

Twenty-seven samples were examined in thin section with the polarized-light optical microscopy for petrography following the nomenclature and classification of Folk (1980), and Zuffa (1980). The quantification of sandstone mineralogy was achieved by counting 400–500 points per thin section following the procedures described in Dickinson (1970), and Ingersoll et al. (1984). Sandstone framework components were divided into the four petrographic groups defined by Zuffa (1980, 1985): non-carbonate extrabasinal (NCE), carbonate extrabasinal (CE), non-carbonate intrabasinal (NCI), and carbonate intra-basinal (CI). A Q–F–L* ternary plot was used to classify the different sandstone types, where L* means fine-grained rock fragments, including carbonate extraclasts-CE.

Mineralogical assemblages of the whole-rock and <2 μm grain-size fraction (clay fraction hereafter) of 63 samples collected in the studied successions were examined by X-ray diffraction to deduce the origin of inherited mineral phases from source areas that fed the basin and possible evidences of synsedimentary tectonics overprinting. The crystalline-powder technique was used for mineral identification in the whole-rock samples. For the non-calcareous clay fraction, four oriented mounts on glass slides per sample were prepared according to methodology by Croudace and Robinson (1983), Holtzapffel (1985), and Moore and Reynolds (1997). A PANalyticalX'Pert Pro ® diffractometer (Cu–Kα radiation, 45 kV, 40 mA) equipped with an X'Celerator solid-state lineal detector was used to obtain the diffraction patterns by a continuous scan from 3° 2θ to 60° 2θ, with a 0.01° 2θ resolution. The Xpowder ® program (Martín-Ramos et al., 2012) was used to evaluate the semi-quantitative mineral composition of whole-rock and clay-fraction samples. The reflections and reflecting powers of Biscaye (1965), and Holtzapffel (1985) were used to identify and quantify the mineral phases. Replicate analyses of a few selected samples gave a precision of ±3 % (2σ). Based upon the X-ray diffraction technique, the semi-quantitative evaluation of each mineral phase (in weight percent, wt% normalized to 100 %) has an accuracy of ~5 %. The parameters examined were (i) the ratio of intensities of the Qtz(001):Qtz(101) peak areas of quartz (Qtz(001):Qtz(101) ratio hereafter) in the whole-rock diffractograms, to discern authigenic quartz from secondary quartz in the absence of a volcanic component (Eslinger et al., 1973); (ii) the ratio of intensities of the Sme(003):Sme(002) peak areas of smectite (Sme(003):Sme(002) ratio hereafter) from ethylene-glycol solvated clay-fraction diffractograms, to differentiate dioctahedral and trioctahedral smectites (Hunziker, 1986; Drits et al., 1997; Moore and Reynolds, 1997; Moiroud et al., 2012); and (iii) the ratio of intensities of the Ill(002):Ill(001) peak areas of illite (Ill(002):Ill(001) ratio hereafter) from decomposed air-dried clay-fraction diffractogram, to discern authigenic from mature illite (Hunziker, 1986; Drits et al., 1997). The smectite+kaolinite:illite (S + K:I) ratio changes were used as a proxy of relative proximity of the source area over time. In open marine environments, the different hydrodynamic behaviour of detrital clay minerals determines their displacement capability to naturally segregate and their possibility for distant transport (Gibbs, 1977). This property can indicate the proximity to the source area (Thiry and Jacquin, 1993; Clark et al., 2009), with implications for palaeogeographic modelling (Dou et al., 2010). In sedimentary basins with a source area composed of aluminic-magnesic silicate minerals, the typical clay-mineral segregation occurs in the following order (from nearshore to offshore): chlorite, illite, kaolinite, random illite-smectite mixed-layer, and smectite (Gibbs, 1977; Patchineelam and de Figueiredo, 2000). The comparison of S + K:I ratio changes with the global sea-level curves enable to relate proximity changes to global eustasy and/or local synsedimentary tectonics (Daoudi et al., 1995; Alcalá et al., 2013a, 2013b). The use of the above X-ray parameters helps to disambiguate tectonics influences overprinting inherited mineralogy.

3. Results

3.1. Stratigraphy

This section is devoted to describe the essential litho- and biostratigraphy features of the studied Rif sectors and the reconstructed successions (Logs 1 to 21) represented in the Figs. 1 and 2. The macro-scale structural analysis carried out in each studied sector, useful for establishing the relationships between tectonic units and style of tectonic deformation, is reported in the Supplemenatry Material A1. The whole stratigraphic description, including location of Logs and thickness of the defined intervals is in the Supplementary Material A2. The whole information about the planktonic foraminifera and calcareous nannoplankton assemblages recognized in from the studied successions is reported in the Supplementary Material A3. This section is arranged in sub-sections according to the main sub-domain of the western External Rif Zone (Internal Intrarif, Extrnal Intrarif, Mesorif and Prerif). For each sub-domain the main stratigraphic features will be presented using the most representative studied logs.

3.1.1. Internal Intrarif

The Logs 1 to 5 belonging to the External Tanger Unit while the Logs 6 to 8 belonging to the Loukkos Unit both of the Internal Intrarif, were examined (Figs. 1; 2). In this sub-domain a synthetic and representative succession was composed with the Jebel Soukna (Log 5), Dehar Sidi Abdalah (Log 3), Mediar (Log 4), Saf Haman (Log 1) and Aïn Kob (Log 8) successions, from bottom to top, as follows:

The top of the Cretaceous succession is well represented in the 220-m-thick of the Jebel Soukna (Log 5). This succession includes three stratigraphic intervals. The 90-m-thick Interval 1 includes blackish to gray-brownish, monotonous and sometimes scaly silt. The 55-m thick Interval 2 is mainly characterized by calcarenite and sand intercalations, and by two slumps, thus indicating a synsedimentary tectonic activity. After 25 m of covered interval, the log ends with 50 m of dark silt with rare intercalations of calcarenites (up to 1-m thick) and centimetric sandstones (Interval 3). Also, the interval 1 of the Log 3 (Dehar Sidi Abdalah) shows similar Cretaceous lithofacies. In both cases, this succession yields upper Cretaceous planktonic foraminifer assemblages (*Rosita fornicata* and *Globotruncanita calcarata*). The Eocene succession is represented by 35 m-thick of the Interval 2 (Log 3). This last interval rests on an unconformity boundary and is made up of stratified greenish marls and silicified grayish limestone marls with chert nodules, which identifies the 'Suessonien' regional marker-unit. It contains frequent radiolarians, agglutinated foraminifera, and more rarely calcareous planktonic and benthic foraminifera. In the lower part (samples 52–53/13) the presence of *Acarinina soldadoensis*, *Acarinina angulosa*, and *Morozovella aragonensis* (for formal names, see also biostratigraphic tables in Supplementary Material A3) suggests that the 'Suessonien' marker-bed could start during the upper Ypresian at least. The 5-m-thick Interval 3 (samples 54–58/13) includes a totally deformed slump of 3-m-thick sandwiched between two minor tectonic contacts. Planktic microfauna made up of *Morozovelloides crassatus, Subbotina frontosa*, *Pseudohastigerina micra*, and *Turborotalia possagnoensis* in coexistence with *M. aragonensis* characterizes the lower Lutetian. The succession ends with 2 m of 'Suessonien' barren lithofacies. The upper part of the Eocene-lower part of the Oligocene succession is represented by two intervals of the Log 4 (Mediar), tectonically overrided by a Numidian-like Unit slice. In particular the 50-m-thick (Interval 1 of this log) consists of greenish marls and silicified calcareous marls also corresponding to the 'Suessonian' regional marked-bed. The presence of *M. crassatus, Turborotalia pomeroli, Globigerinatheka subconglobata*, and *Globigerina eocaena* delimits the biostratigraphic interval E10–E13 (upper Lutetian–Bartonian). The 100-m-thick Interval 2 is constituted by brownish silt

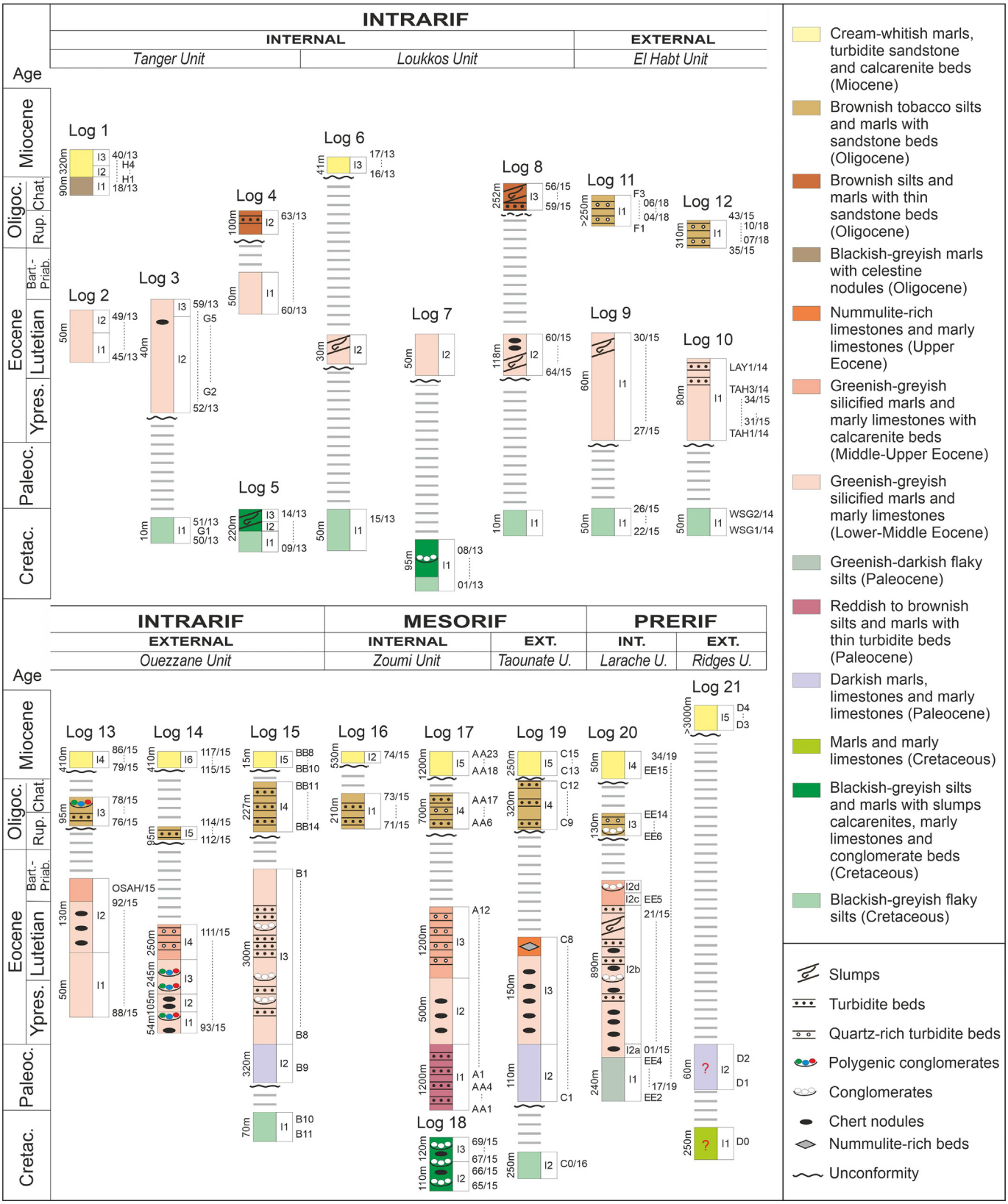

Fig. 2. Reconstructed stratigraphic successions ordered by Domain, sud-Domain, and Sector as follows: (i) Internal Intrarif, External Tanger Unit, Tanger Sector: Saf Haman (Log 1), Oulad Ziane (Log 2), Dehar Sidi Abdalah (Log 3), and Mediar (Log 4); (ii) Internal Intrarif, External Tanger Unit, Chauen Sector: Jebel Soukna (Log 5); (iii) Internal Intrarif, Loukkos Unit, Chauen Sector: Taïjoute (Log 6), Oued Tazarine (Log 7), and Aïn Kob (Log 8); (iv) External Intrarif, El Habt Unit, Asilah Sector: El Arba Aycha (Log 9), Tahar (Log 10), Dmina (Log 11), and Mezgalef (Log 12); (v) Internal Prerif, Larache Unit, Asilah Sector: Sidi M'raït (Log 20); (vi) External Intrarif, Ouezzane Unit, Ouezzane Sector: Sidi Ameur (Log 13), Douar Ahel Chane (Log 14), and Oulad Ktir (Log 15); (vii) Internal Mesorif, Zoumi Unit, Zoumi Sector: Oued Anngouch (Log 16), Fej el Hanout (Log 17), and Aïn Bou Hassane (Log 18); (viii) External Mesorif, Izzarene Unit, Ourtzarh Sector: El Mizab (Log 19); (ix) External Prerif, Ridges Unit, Ridges Sector: Talaghza (Log 21). Location of the studied sectors is in Fig. 1. The whole stratigraphic data and descriptions in the Supplemenatry Material A2. The whole information about the planktonic foraminifera and calcareous nannoplankton assemblages is in the Supplementary Material A3.

and marl beds alternating with 10–20-cm thick turbidite sandstone layers. The planktonic assemblage shows *G. ampliapertura, "G." increbescens, Neogloboquadrina opima*, *G. eocaena*, and *Globigerina corpulenta,* referable to the biozone O2 (middle Rupelian). Finally, the transition Oligocene-Miocene was recognized in the Saf Haman succession (Log 1) divided into two intervals. The lower 90-m-thick (Interval 1) of this log includes homogeneous marls with marly limestone intercalations containing *Globigerinoides primordius* and *Globorotalia* cf. *kugleri*, which characterize the top of the Chattian. The upper 50-m-thick (Interval 2) includes bioturbated marls with episodic intercalations of laminated and lenticular limestones, yielding typical morphotypes of *Globorotalia kugleri* (bed 21/13) that indicates the beginning of the Aquitanian. The Oligocene *p.p.* is also represented in the upper part of the Aïn Kob succession (Log 8) that shows slightly different lithofacies. The >250-m-thick Interval 3 of the Log 8 is made by alternating brownish silt and centimetric to decametric turbidite sandstone beds with slumps. In the lower part (sample 57/15), the presence of planktonic foraminifera (*P. micra, Chiloguembelina cubensis, Globigerina ampliapertura, and "Globigerina" increbescens*) constraints to the biozone O1 (early Rupelian) while in the uppermost part (sample 56/15) the association *G. ciperoensis, G. eocaena*, and *G. corpulenta* is attributed to the O5–O6 zonal interval (Chattian).

3.1.2. External Intrarif

The Logs 9 to 12 belonging to the El Habt Unit while the 13 to 15 belonging to the Ouezzane Unit were studied (Figs. 1; 2). Nevertheless, the most representative succession of this sub-domain is well represented in the Oulad Ktir succession (952-m-thick, Log 15), includes five intervals. The lower 70-m-thick (Interval 1) consists of homogeneous blackish silt that at the top provided a Maastrichtian microfauna. Above an unconformity the Interval 2 (320-m-thick) consists of yellowish-white marls with intercalations of marly-limestones. The lowest sample B9/16 provided planktonic foraminifera of the uppermost part of the lower Paleocene (*Parasubbotina pseudobulloides, Praemurica inconstans, Praemurica uncinata and Globanomalina compressa*). A stratigraphic gap corresponding to an unspecified part of the lower Paleocene was recognized. The 300-m-thick Interval 3 is stratigraphically continuous, shows cream-colored marls interbedded with well-stratified fine sandstones (5–20-cm thick), and occasional polygenic conglomerates beds (0.6–1-m thick) with cherty intraclasts and slumps. It also includes marly-limestones of "Suessonien" lithofacies, micritic limestones and calcarenites. The planktonic foraminifera of the samples B8–1/16 reveal a continuous sedimentation from the lower Ypresian to the lower Bartonian. As in the case of the Logs 4, 8 and 20, the upper part of the Eocene is marked by an unconformity with stratigraphic gap extending from the upper Eocene (Bartonian *p.p.* to Rupelian *p.p.*) to the lower Rupelian *p.p.* The 247-m-thick Interval 4 represents the Oligocene *p.p.* (upper Rupelian–lower Chattian) succession. It consists of homogeneous brownish (tobacco) silt with scarce turbidite quartz-rich sandstones (sandstone:silt ratio about 5:95). Samples B14–11/16 suggest a continuous sedimentation from the upper Rupelian to the lower Chattian. A further unconformity with a stratigraphic gap extending from the top of the Chattian *p.p.* to the Aquitanian *p.p.* marks the base of the >15-m-thick Interval 5. It is represented by marls with interbedded marly limestones. The presence of *G. altiaperturus* in the basal sample BB14/18 reveals that the Interval 5 begins in the lower Burdigalian.

3.1.3. Mesorif

The Logs 16 to 18 belonging to the Zoumi Unit while the Log 19 belonging to the Taournate Unit, were studied (Figs. 1; 2), but the most representative succession of this sub-domain is well represented in the 4800-m-thick Fej el Hanout succession (Log 17) that includes five intervals. The 1200-m-thick Interval 1 consists of stratified blackish scaly silt, sometimes marly, with intercalations of thin-bedded limestones and fine-grained sandstones. The sandstone:silt ratio is about 20:80. The several slumps checked at the top represents the oldest Paleogene deposits recognized in the overlying External Rif successions. The planktonic foraminifera (samples AA1–4/18 and A1–2/16) indicate the zonal interval Pα–P2 (lower Paleocene), while at the top (sample A4/16) the presence of *M. velascoensis* identifies the first upper Paleocene deposit. The 400-m-thick Interval 2 lies stratigraphically above the previous one and shows limestones and marly limestones characterized by well-stratified chert nodules, interspersed with gray-yellow marls corresponding to the 'Suessonian' marker-bed. The interval shows a poor microfauna, in particular in the lower part (samples 5–8/16) attributed to the Paleocene–Eocene transition, where only rare agglutinated foraminifera and siliceous teeth are preservated. The upper part (samples A9–11/16) shows a more varied Ypresian and lower Lutetian microfauna. The 1300-m-thick Interval 3 lies above the previous one and consists of alternating cream-colored marls and silt, and turbidite sandstones. In the lower part, the planktonic foraminifera of sample A12/16 restricts to the zonal interval E10–E11 (middle–upper Lutetian), while the upper part reaches the Bartonian, similarly to the Eocene deposits checked in other studied Logs. Once again, the top of the Eocene deposits is marked by an unconformity with a stratigraphic gap extending from the upper Eocene to the lower Rupelian. The 700-m-thick Interval 4 lies above this latter unconformity and consists of alternating brownish silt and turbidite quartz-rich sandstones. The rich planktonic foraminifera association provides an accurate chronology that shows a continuous deposition through the middle Rupelian (samples A6–10/16), upper Rupelian (samples A11–13/16), and uppermost Rupelian–early Chattian (samples A14–17/16). The 1200-m-thick Interval 5 consists of a lower Miocene turbidite silty–marly/sandy calcarenitic succession (samples AA18–23/18). Although this interval rests in apparent lithostratigraphic continuity above the previous interval, a short gap affecting the Oligocene to Miocene transition cannot be excluded. The entire succession shows a regressive trend, as indicated the upward increase in thickness of sandstones. The opposite sand content decreasing evolution observed in the upper 150 m of the succession may be interpreted as the beginning of a transgressive trend. The succession is interrupted by a tectonic contact (thrust), where the thrust sheet is represented by the Loukkos Unit.

3.1.4. Prerif

The succession of the Log 20 represents the Larache Unit while the Log 21 documents the Ridges Unit (Fig. 1; 2). The most representative succession of this sub-domain is well represented in Sidi M'raït (Log 20) as follows:

This 1390-m-thick studied succession was divided into four intervals. The 240-m-thick Interval 1 (samples EE2–4/18) consists of greenish, scaly and homogeneous silt containing lower Paleocene primitive planktonic foraminifera (*Eoglobigerina eobulloides, Globanomalina archeocompressa*, and *Praemurica taurica*). The 960-m-thick Interval 2 conformably lies above the previous one. In this interval, four sub-intervals were distinguished. The 70-m-thick sub-Interval 2a (sample 01/15) shows stratified calcareous marls and whitish marls with intercalated homogeneous limestones with chert nodules, and planktonic foraminifera belonging to the lower Paleocene (*P. pseudobulloides, P. inconstans*). The 550-m-thick sub-Interval 2b is made up of siliceous marls and marly limestones, containing limestone, arenite and conglomerate beds, the latter with extraformational calcareous clasts and interpreted as olistostromes. The lower part (samples 2–8/15) is barren in microfauna and contains just *Microcodium*-like structures and rare siliceous teeth but the occasional presence of *M. velascoensis* (sample 4/15) makes it possible to refer these deposits to the upper Paleocene–lowermost Ypresian. Upwards, assemblages characterizing the Ypresian to upper Lutetian are reconigzed (samples 9–12/15). The 100-m-thick sub-Interval 2c is constituted by marls and marly limestones, turbidite sandstones, and slumps. The 340-m-thick sub-Interval 2d is represented by marls and marly-limestones, limestone beds and extrabasinal calcareous conglomerates (olistostromes). The sample EE5/18 contains an assemblage of planktonic foraminifera (such as *M. crassatus,*

Hantkenina dumblei, Turborotalia pomeroli) restricted to the Zone E11 of the Lutetian–Bartonian transition. The 130-m-thick Interval 3 is deposited above an unconformity surface (stratigraphic gap about 12 Ma) and is constituted by brownish pelites with intercalations of turbidite quartz-rich sandstones and conglomeratic beds. The pelites yielded a rich microfauna of planktonic foraminifera, showing a continuous sedimentation through the middle–upper Rupelian (samples EE6–14/18). The 60-m-thick (at least) Interval 4 is deposited above a second unconformity surface (undeterminable stratigraphic gap). It is constituted by brownish silt with intercalations of turbidite quartz-rich sandstones (sandstone:silt ratio about 15:85) and lower Miocene *p.p.* whitish marls.

3.2. Petrography

This section describes the essential petrographic findings of the studied Logs in the Intrarif (Logs 9, 11, 12 and 14), Mesorif (Logs 16, 17 and 19), and Prerif (Log 20) sub-Domains (Figs. 1; 2; 3). The detailed petrographic results are in the Supplementary Material A4.

3.2.1. Detrital suites of the Intrarif sub-Domain

In this sub-domain, terrigenous deposits are classified by the NCE–CI–CE diagram (Zuffa, 1980) as carbonate intrarenites (samples 24/15 and 38/15) and non-carbonate extrarenites (sandstones) (samples F3, 39/15, 105/15 and 112/15) (Fig. 3A). The sample 24/15 (Log 9; Eocene) is a finely laminated biomicrite with abundant fine-sand grains (20–60 μm), mainly monocrystalline quartz and glauconite. Bioclasts are filled by calcite and/or ferruginous cement. Matrix is mainly composed of micrite, with variable amounts of clay minerals and Fe-oxides. Sample 38/15 (log 12; Oligocene) is a poorly sorted quartz-rich lithoclastic grainstone/rudstone where bioclasts are relatively large (>1 mm). Quartz grains (50–500 μm), both mono- and polycrystalline, are subrounded to subangular. Some quartz grains contain anhydrite inclusions. Recycled or second-cycle quartz (with syntaxial overgrowths) are recognized. Glauconitic grains (50–100 μm) are also present. Lithoclasts mainly consist of sedimentary rock fragments. Micrite matrix is relatively scarce. Calcite cement is microsparitic. Grain-coating and pore-filling cements of Fe oxides/hydroxides are also present. Samples 39/15 (Log 12; Oligocene), 105/15 (Log 14; Eocene), and F3 (Log 11; Oligocene) are classified as fine- to medium-grained sublitharenites according to the Q–F–L diagram (Folk, 1980) (Fig. 3B). On the other hand, sample 112/15 (Log 14; Oligocene) is classified as a fine- to medium-grained litharenite. These arenites are mainly composed of monocrystalline quartz, carbonate rock fragments, and bioclasts. Polycrystalline quartz, feldspars, glauconite, and opaque minerals are also present. Recycled or second-cycle quartz (with syntaxial overgrowths) are recognized. Both quartz and feldspar grains are commonly corroded (replaced by carbonates). Polymictic sandstone-microbreccia (sample 59/15; Log 3; Oligocene) is composed of angular (0.2–3 mm) grains mainly of quartz (monocrystalline and polycrystalline), plagioclase, dolomite, sedimentary, and volcanic rock fragments in a micritic matrix. Limestone lithofacies (samples DSA-1–3; Log 3; Eocene) are mainly wackestone-packstones with some monocrystalline, variably rounded quartz (20–150 μm), glauconite (about 100 μm), and opaque mineral (about 50 μm) grains. Locally, euhedral dolomite crystals (40 μm), are also recognized. Usually globigerinides fragments are partly silicified.

3.2.2. Detrital suites of the Mesorif sub-Domain

Two types of sandstones are present in this domain: Non-carbonate extrarenites and hybrid arenites. The extrarenite sandstones characterized by the dominance of siliciclastic grains (NCE) over carbonate grains are classified as litharenites (samples A13, Eocene, and AA7, AA15, Oligocene log 17). Samples AA15 and A13 are laminated moderately to well-sorted fine-grained (25–150 μm) laminated litharenites. On the other hand, sample AA7 is a coarser-grained (50–300 μm) poorly sorted litharenite. These arenites are mainly composed of monocrystalline quartz, carbonate rock fragments and bioclasts. Polycrystalline quartz, feldspars, glauconite, and opaque minerals are also present. As in Prerif extrarenites, recycled or second-cycle quartz (with syntaxial overgrowths) are recognized, and silicate grains are commonly corroded (replaced by carbonates). Hybrid arenites in Oligocene samples 73/15

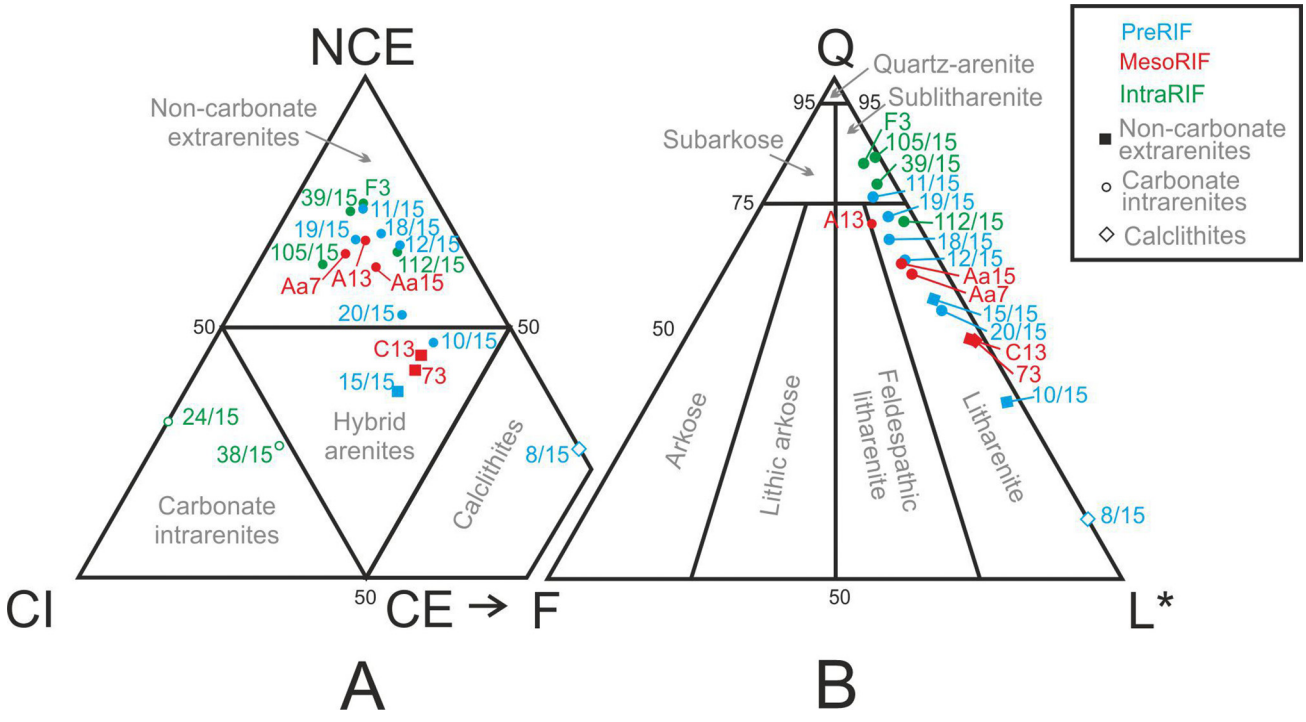

Fig. 3. Petrographic analysis in the Intrarif (Logs 9, 11, 12 and 14), Mesorif (Logs 16, 17 and 19), and Prerif (Log 20) sub-Domains. Composition of Paleogene arenites. (A) First-order compositional plot, as NCE—Non-Carbonate Extrabasinal grains, CE—Carbonate Extrabasinal, and CI—Carbonate Intrabasinal. (B) Diagram of the main composition, as Q–Quartz, F–Feldspar, and L*–Lithic Fragments including carbonate rocks. The detailed petrographic results are in the Supplementary Material A4.

(Log 16) and C13 (Log 17) show 50–60 % carbonate grains (CI + CE) (Fig. 3A) and also are classified as litharenites in the Q–F–L*diagram. Framework is mainly composed of monocrystalline quartz, sedimentary rock fragments (wackestone, packstone), and bioclasts. Subrounded to Subangular monocrystalline quartz (75–500 μm) and composite fine-grained quartz are the main siliciclastic grain types. Recycled or second-cycle quartz (with syntaxial overgrowths) are recognized. Feldspars (plagioclase), glauconite, and opaque minerals are also present with sizes in the 50–250 μm range. Both quartzose and feldspar grains are commonly corroded (replaced by carbonates). Limestone lithofacies (sample AA12; Log 17; Oligocene) are mainly mudstone-wackestones with some monocrystalline subangular quartz (20–75 μm), feldspar and metamorphic rock fragments (50–200 μm).

Samples 18–20/15 (Log 20; Eocene) are classified as medium- to coarse-grained poorly-sorted litharenites. These arenites are mainly composed of subangular to subrounded monocrystalline quartz, carbonate rock fragments, and partially silicified bioclasts. Polycrystalline quartz, feldspars, glauconite, and opaque minerals are also present. Recycled or second-cycle quartz (with syntaxial overgrowths) are recognized. Both quartz and feldspar grains are commonly corroded (replaced by carbonates). On the other hand, sample 11/15 (Log 20; Eocene) is classified as fine- to medium-grained poorly-sorted sublitharenite, mainly composed of subrounded to angular monocrystalline quartz grains, and carbonate rock fragments. Polycrystalline quartz, feldspars, glauconite, and opaque minerals are also present. Recycled or second-cycle quartz are locally recognized. Both quartz and feldspar grains are commonly corroded (replaced by carbonates).

3.2.3. Detrital suites of the Prerif sub-Domain

As in the Mesorif sub-domain, hybrid arenites (samples 10/15 and 15/15; Log 20; Eocene) in this sub-domain are classified as hybrid arenites (NCI-rich non-carbonate intrabasinal grains as galuconite are relatively abundant) in the NCE-CI-CE diagram (Fig. 3A) and as litharenites in the Q–F–L*diagram (Fig. 3B). Framework is mainly composed of monocrystalline quartz, sedimentary rock fragments (packstone, grainstone, arenite), and bioclasts. These grains are commonly corroded (replaced by carbonates). Subrounded to Subangular monocrystalline quartz (75–500 μm) is the main siliciclastic grain types. Recycled or second-cycle quartz (with syntaxial overgrowths) are recognized. Sample 8/15 (Log 20; Eocene) is mainly composed by extrabasinal coarse (0.25–2 mm) carbonate grains and has been classified as a calcilithite in the NCE–CI–CE diagram. This sample is poorly-sorted with subangular to subrounded grains. Sedimentary lithic fragments (mainly bioclastic limestones, fine-grained arenites, shales and macrocrystalline idiotopic dolosparites) dominate the grain framework: quartz (partially replaced by carbonate), glauconite, opaque minerals and bioclast fragments are also present. Carbonate grains are partially silicified. Poorly-sorted polymictic sandstone-microbreccias (samples 16–17/15; Log 20; Eocene) are mainly composed of subrounded to angular (0.1–3 mm) monocrystalline and polycrystalline quartz grains and rock fragments. Bioclasts and opaque grains are also recognized. Matrix consists of micritic to microsparitic mosaics.

Post depositional modification during burial is evidenced in most of the studied samples by: (i) microsparitic and/or poikilotopic calcite cementation; (ii) compactation manifested by mechanical deformation of ductile carbonate and glauconite grains, fracturation of grains, and the presence of long and concave-convex boundaries between quartz grains; (iii) corrosion (replaced by carbonates) of quartz and feldspar clasts; and (iv) local clay pore filling and replacement (epimatrix after feldspar).

3.3. Mineralogy

This section describes the essential findings of the average whole-rock and clay fraction mineralogy (in %) of the studied samples in the Tanger (Logs 1 and 3), Ouezzane (Logs 13 and 14), Zoumi (Log 17), and Asilah (Log 20) Sectors in the Intrarif, Mesorif, and Prerif sub-Domains (Figs. 1; 2; 4). The detailed mineralogical results are in the Supplementary Material A5.

3.3.1. Clay mineral associations in the Intrarif sub-Domain

This sub-domain is divided into 'Internal Intrarif', well represented in the Tanger Sector, and 'External Intrarif' outcropping in the Ouezzane Sector. In the Tanger Sector (Fig. 2), the mineralogy of mudstones in the samples G2–G3/16 (Log 3; Ypresian), G4–G5/16 (Log 3; Lutetian), and H1–H2/16 (Log 1; Chattian) (Fig. 4) characterizes the Ill+Kln + (I-S) ± Sme + Chl clay-mineral association in all lithofacies, and the Sme + (I-S) ± Ill+Kln clay-mineral association in the sample H2/16 (Log 1; late Chattian). The dimensionless (S + K):I ratio is 0.25–0.30 (Log 3; Ypresian), 0.47–0.54 (Log 3; Lutetian), 2.23 (sample H1; Log 1; early Chattian), and >10 (sample H2; Log 1; late Chattian). These figures seem to evidence a progressive increasing of distality from Ypresian to Chattian (Fig. 4). The Qtz(001):Qtz(101), Sme(003):Sme(002), and Ill(002):Ill(001) ratios (Fig. 4) respectively suggest secondary quartz, since Qtz(001)/Qtz(101) ratios lower and higher than 0.30 identify secondary and authigenic quartz, respectively (Eslinger et al., 1973); dioctahedral and trioctahedral smectites in similar proportion, since inherited Mg-rich phases (dioctahedral) like montmorillonite and beidellite give ratios <1 and Al-rich phases (trioctahedral) like nontronite and saponite give ratios >1 (Moore and Reynolds, 1997; Moiroud et al., 2012); and ratios <0.30 are attributed to mature illite and ratios >0.30 identify inherited micas from low-grade metamorphic rocks (Drits et al., 1997).

In the Ouezzane Sector in the External Intrarif (Fig. 2), the mineralogy of mudstones in the samples 88–89/15 (Ypresian), 90/15 (Lutetian), 76/15 (Rupelian), and 77–78/15 (Chattian) in Log 13 (Fig. 4) characterizes the Ill+Sme + (I-S) clay-mineral association in all lithofacies. In Log 14 (Fig. 4), the mineralogy of mudstones in the samples 93–100/15 (Ypresian) characterizes the Ill+(I-S) ± Sme + Kln clay-mineral association, while the Ill+Kln ± (I-S) + Sme + Chl clay-mineral association is characterized in the samples 101–111/15 (Lutetian) and 112–114/15 (Rupelian). The (S + K):I ratio is 0.38–0.55 in Log 13 and 0.14–2.68 in Log 14, thus evidencing more distality conditions in the former one (Fig. 4). The Qtz(001):Qtz(101), Sme(003):Sme(002), and Ill(002):Ill(001) ratios (Fig. 4) respectively suggest secondary quartz with some occurrence of authigenic quartz in the samples 90–92/15 (Log 13; Lutetian), and 110/15 and 113–116/15 (Log 14; Rupelian); dioctahedral smectite with trioctahedral smectite in the samples 78/15 (Log 13; Chattian) and 110/15 (Log 14; Lutetian) and 113–114/15 (Log 14; Rupelian); dioctahedral smectite with trioctahedral smectite in the samples 77/15 (Log 13; Chattian), 98–100/15 (Log. 14; Ypresian), and 101/15 and 110/15 (Log. 14; Lutetian); and inherited illite with mature illite in some samples in the Lutetian lithofacies in Log 14. In Logs 13 and 14, the identification of authigenic illite (Ill(002):Ill(001) ratios >0.40) in late Ypresian, early Lutetian, and Oligocene could suggest incipient low-grade (burial) metamorphism (anchizone) (Nieto et al., 1996). However, the presence of smectite and mixed layers I-S in all samples restrict this range to weak burial diagenesis at most (Lanson et al., 2009; Moiroud et al., 2012; Alcalá et al., 2013a, 2013b).

3.3.2. Clay-mineral associations in the Mesorif sub-Domain

This sub-Domain is represented in the Zoumi Sector (Log 17) (Fig. 2). The mineralogy of mudstones in the samples A1–A4 (Paleocene), A5–A10 (Ypresian), A11–A12 (Lutetian), AA6–AA7 (Rupelian), and AA15–AA17 (Chattian) (Fig. 4) characterizes the Ill+(I-S) ± Sme + Kln clay-mineral association in all lithofacies. The (S + K):I ratio varies in the 0.64–3.71 range, with the typical lowest values in Ypresian and the highest in Rupelian and Chattian (Fig. 4). The Qtz(001):Qtz(101), Sme(003):Sme(002), and Ill(002):Ill(001) ratios (Fig. 4) respectively suggest variable amounts of authigenic (samples AA16–AA17; Chattian) and secondary quartz, dioctahedral (ratio < 1) and trioctahedral (ratio > 1) smectite, and inherited (ratio > 0.30) and mature (ratio < 0.30, some samples in early Lutetian and

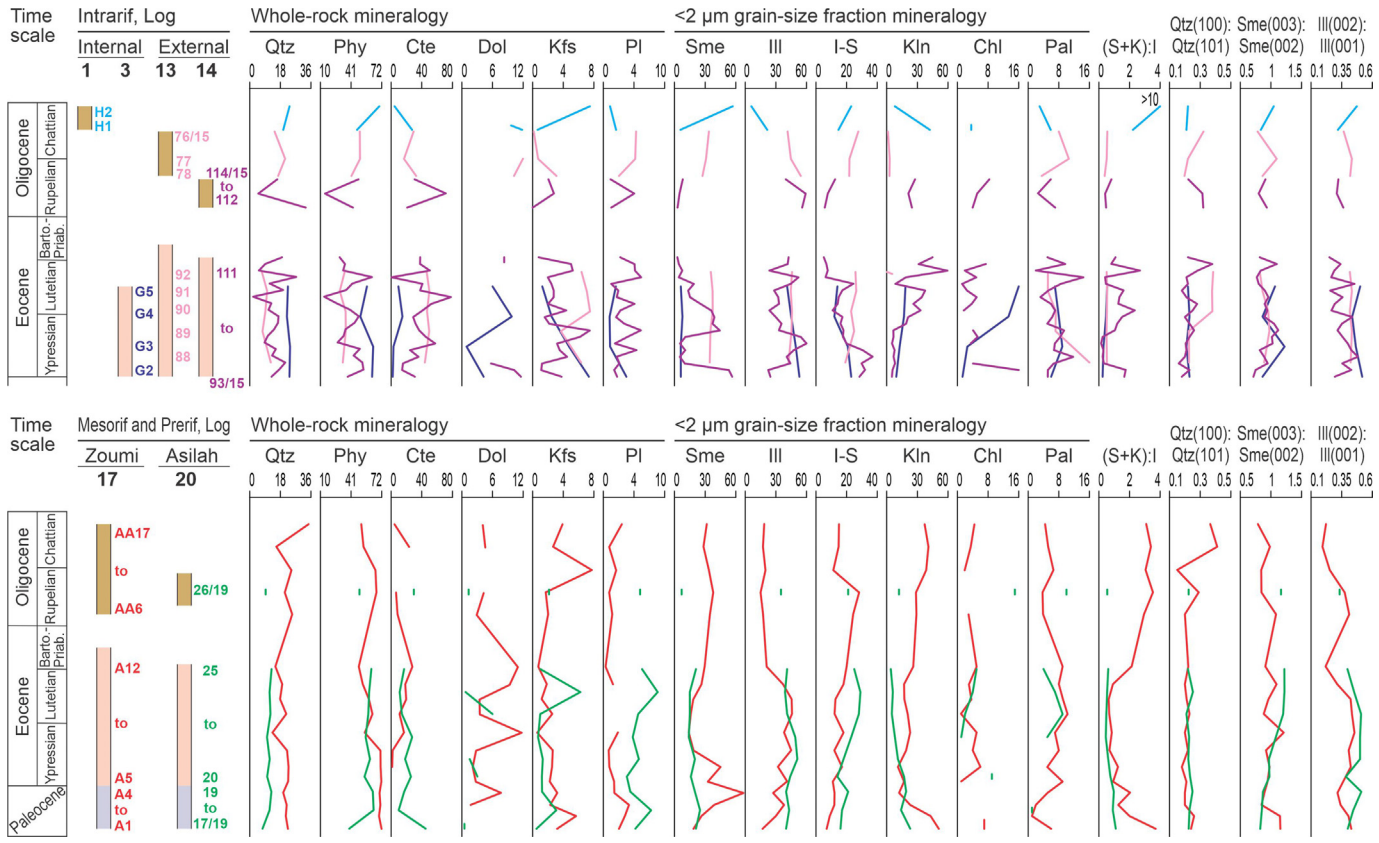

Fig. 4. Whole rock and the <2 μm grain-size (clay-fraction mineralogy in wt%) of mudstones sampled in the Log 1 (Saf Hamam succession, cian lines) and Log 3 (Dear Sisi Addallah succession, dark blue lines) from the Tanger Sector, Log 13 (Sidi Ameur succession, pink lines) and Log 14 (DouarAhel Chane succession, purple lines) from the Ouezane Sector, Log 17 (Fej el Hanout, red lines) from the Zoumi Sector, and Log 20 (Sidi M'raït, green lines) from the Asilah Sector. The dimensionless (smectite+kaolinite):illite ((S + K):I) ratio, and the intensities ratio of the Qtz(001):Qtz(101) peak areas of quartz, Sme(003):Sme(002) peak areas of smectite from ethylene-glycol solvated clay-fraction, and Ill(002):Ill(001) peak areas of illite are also included. Qtz—quartz, Phy—phyllosilicates, Cte—calcite, Dol—dolomite, Kfs—K-feldspar, Pl—plagioclase, Oct—opal CT, Sme—smectite, Ill—illite, I-S—random mixed layer illite-smectite, Kln—kaolinite, Chl—chlorite, and Pal—palygoskite. The detailed mineralogical results are in the Supplementary Material A5.

Chattian) illite. As in the Ouezzane Sector (Logs 13 and 14), the identification of authigenic illite in early Lutetian and Chattian could suggest incipient low-grade (burial) metamorphism (anchizone) (Nieto et al., 1996), although the presence of smectite and mixed layer I-S in all samples restrict also this range to weak burial diagenesis at most (Lanson et al., 2009; Moiroud et al., 2012; Alcalá et al., 2013a, 2013b).

3.3.3. Clay-mineral associations in the Prerif sub-Domain

This sub-Domain is represented in the Asilah Sector (Log 20) (Fig. 2). The mineralogy of mudstones in the samples 17–19/19 (Paleocene) and 20–22/19 (Ypresian) (Fig. 4) characterizes the Ill+(I-S) ± Sme + Kln clay-mineral association in all lithofacies, while the Ill+(I-S) ± Sme + Kln + Chl clay-mineral association is characterized in the samples 25/19 (Lutetian), and 26/19 (Rupelian). The (S + K):I ratio (Fig. 4) decreased from 0.91 to 1.10 in the samples 17–19/19 (Paleocene) to 0.54 in the sample 26/19 (Rupelian), thus evidencing decreasing distality conditions over time. The Qtz(001):Qtz(101), Sme(003):Sme(002), and Ill(002):Ill(001) ratios (Fig. 4) respectively suggest secondary quartz in all lithofacies; dioctahedral (Paleocene and early Ypresian lithofacies) and trioctahedral (late Ypresian, Lutetian, and Rupelian lithofacies) smectites; and inherited illite from low-grade metamorphic rocks in all lithofacies (Drits et al., 1997).

4. Main unconformities and depositional sequences

The correlation of all the reconstructed successions, together with their tectonic position in the different examined sectors, allowed proposing a first stratigraphic framework of the Paleogene stratigraphic record of the western External Rif Zone (Fig. 5). The reconstructed stratigrahy shows three unconformity surfaces coarsely aligned with (i) the Cretaceous–Cenozoic boundary, with a gap covering the uppermost Cretaceous (in most cases) and/or the Paleocene, and even a part of the lower Eocene; (ii) the Eocene–Oligocene boundary, with a gap extending in most cases from the middle–upper Eocene to the lower Oligocene; and (iii) the Oligocene–Miocene boundary, with a gap corresponding in most cases to the middle–upper Oligocene to lowermost Miocene. The older two unconformities are recognizable in all the examined sectors; they can be considered main unconformities. The most recent unconformity shows a lesser lateral extent; it will be considered a second-order unconformity. On the contrary, the upper one is not represented in the Internalmost Intrarif and probably is a secondary unconcormity. The recognized gaps can be divided into depositional (unrecorded period above the most recent age of the lower stratigraphic unit) and/or erosional (unrecorded period below the oldest age of the upper stratigraphic unit) ones.

These unconformities allow dividing the stratigraphic record into four stratigraphic sequences, as (i) upper Cretaceous; (ii) Paleocene–middle Eocene (Bartonian); (iii) Oligocene *p.p.;* and (iv) Miocene *p.p.* The first three units are represented in almost of the sectors (Fig. 10). Also, the middle Eocene portion of the second unit appears in all sectors, while its Paleocene portion is represented in the outermost sectors only (Ouezzane Unit of the External Intrarif, Mesorif, and Prerif) and is absent both in the Internal Intrarif (Tanger and Loukkos units) and in the External Intrarif (El Habt Unit).

5. Evidences of *syn*-sedimentary tectonics

The analysis of structures related to synsedimentary tectonics recognized in the Paleogene stratigraphic record of the western External Rif

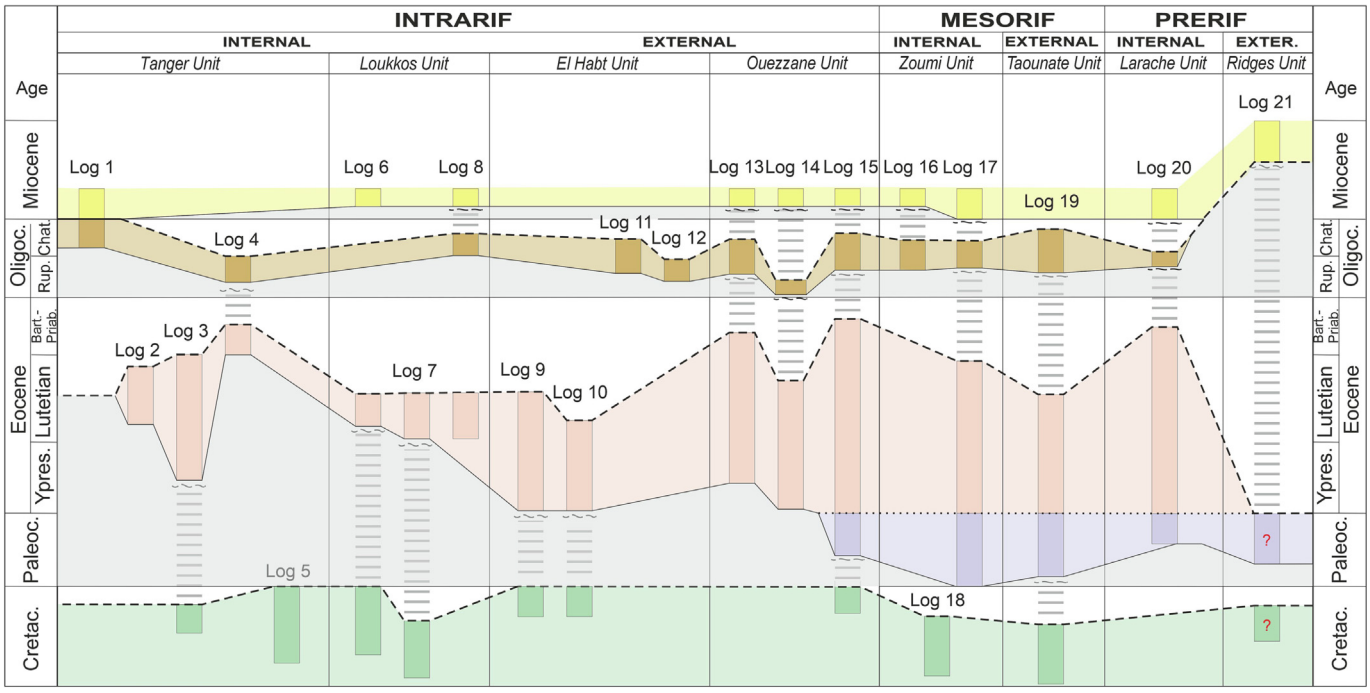

Fig. 5. Paleogene stratigraphic framework of the western External Rif Zone, showing stratigraphic units, unconformities, and depositional vs. erosional gaps.

Zone was based on the following indicators of synsedimentary tectonics (i) Mass flow deposits (tectofacies); (ii) Synsedimentary faults and folds; (iii) Unconformities; (iv) Petrographical and Mineralogical evidences; and (v) Subsidence analysis.

5.1. Mass flow deposits (turbidites, slumps, olistostromes)

5.1.1. Turbidites

They (Fig. 6A–B) may be commonly related to syn-sedimentary tectonic activity affecting the depositional system and controlling the relative proximality/distality of depositional area also. The composition of turbidite beds is mainly related to the type of sediment and source area, which is often an arenitic/calcarenitic supply. Turbidite deposits are in almost all the studied outcrops from the Ypresian upwards and are often associated with slumps and olistostromes. However, turbidites increase from the Oligocene upwards, especially in the external domains. In fact, they are less abundant in the Internal Intrarif, where depositional conditions favored the development of the Eocene 'Suessonien marked-bed' siliceous lithofacies. Turbidites are not exclusively related to synsedimentary tectonics, but these deposits indicate this type of tectonics when they are associated with slumps and olistostromes; these latter occurred especially from the Oligocene onwards.

5.1.2. Slumps

They are systematically present in most of the studied successions from the upper Ypresian onwards (Fig. 6C–D), although they are more abundant from the Oligocene both in the Larache and Ouezzane Units (Internal and External Intrarif, respectively) and Mesorif units. Commonly associated with turbidite successions, these slumps may have been deposited at the base of slopes affected by synsedimentary tectonics, thus causing sediment instability and therefore slumping. At a number of stratigraphic levels, decametric deformed intervals have been interpreted as large sliding masses.

5.1.3. Olistostromes

They are interbedded within turbidite successions, and consist of coarse deposits usually showing a basal erosion surface and a poor internal organization (Fig. 6E–F). Sometimes these deposits are represented by monogenic intra-basinal conglomerates with slightly rounded pebbles, and in other cases are polygenic conglomerates resulting from an extra-basinal supply. Olistostromes occur already from the terminal Ypresian, although they are more abundant from the Oligocene onwards, and usually indicate tectonic instability of the margin/basin system.

5.2. Syn-sedimentary faults and folds

These structures are common in almost of the observed outcrops and were originated during the sedimentation probably by tectonic instatability. They are sealed by undeformed or less deformed strata (Fig. 6G–H). The faults usually show a centimetric to decametric displacement that progressively reduces upwards, and are recognizable in some layers covered by not faulted beds only (Fig. 6G). The observed folds (Fig. 6H) differ from the slump-related folds by its minor deformation and a simpler geometry.

5.3. Unconformities implications on synsedimentary tectonics

The Cretaceous–Cenozoic and Eocene–Oligocene unconformities seem to match with regional deformation phases affecting the western Tethys (Stampfli et al., 2002; Khomsi et al., 2006, 2009; Chalouan et al., 2008; Guerrera and Martín-Martín, 2014; Guerrera et al., 2021). The Cretaceous–Cenozoic unconformity could be correlated to the tectonic inversion (from extension to compression) occurred in the alpine Tethys domains linked to the opening of the South Atlantic Ocean (Stampfli et al., 2002). Instead, the Oligocene–Miocene unconformity seems to coincide with a flexural deformation of the Atlas front (Khomsi et al., 2006, 2009). All these tectonic events affecting the Paleogene successions (Chalouan et al., 2008; Guerrera and Martín-Martín, 2014) can refer to two deformation phases. The latest Cretaceous to early Oligocene tectonic events would be related to the so-called Eoalpine or Alpine *s.s* orogenic phase, which is linked to the closure of the northern branch of the western Tethys and contemporary to the formation of the Alps and the Pyrenees (Guerrera et al., 2021). Most of the above-described deformation recorded in the western External Rif Zone during the Paleogene would represent the imprint (side-effects) of this

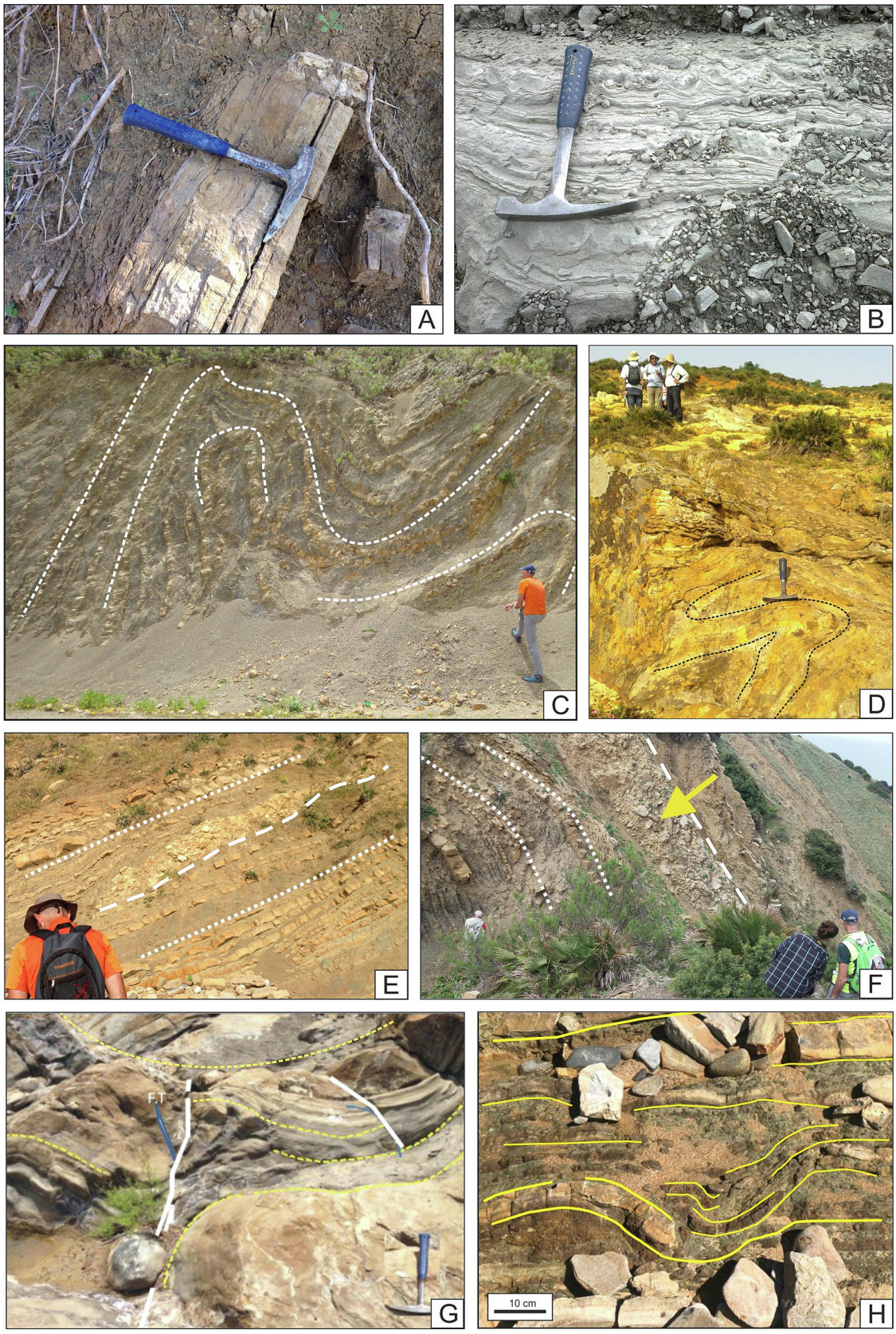

Fig. 6. Sedimentary and tectonic structures supporting synsedimentary tectonics. (A) Eocene turbidite (Log 13); (B) Oligocene turbidite (Log 1); (C) Eocene slump (Log 15); (D) Oligocene slump (Log 12); (E) Eocene mass flow (Log 20); (F) Oligocene mass flow (Log 20); (G) Eocene synsedimentary fault; (H) Eocene synsedimentary fold (Log 20).

orogenic phase in this far area from the main focus of the Eo-Alpine phase. Instead, the late Oligocene and Miocene evolution would be related to the Neoalpine or Maghrebian phase (Guerrera et al., 2021). This phase is linked to the closure of the southern branch of the western Tethys (Maghrebian Flysch Basin; Guerrera and Martín-Martín, 2014; and references therein) and would originate the Maghrebian Chain (Rif, Tell, and Calabria-Peloritani Arc) and most of the Betic Cordillera.

5.4. Petrographical evidences

Modal analyses of non-carbonate extrarenites and hybrid arenites (sandstone samples) of the western External Rif Zone show extrabasinal quartz grains, thus indicating sedimentation from middle to upper rank metamorphic source areas during tectonic rising (Fig. 7A). The intrabasinal quartz grains must be derived from erosion of the local calcarenitic older intervals in areas with active benthic carbonate production. Locally, hybrid arenites dominate (upper Oligocene, Mesorif) and carbonate sedimentary sources (both coeval and non-coeval) must be more important. All samples fall into the 'recycled orogen' tectonic setting (Dickinson et al., 1983) (Fig. 7B). Specifically, the hybrid arenites and calcilithites corresponded to the 'transitional recycled' sub-type, and most of the terrigenous extrarenites to the 'recycled' sub-type.

The existence of second-cycle or recycled quartz grains and abundance of sedimentary rock fragments suggest a recycling origin related to the erosion of older siliciclastic and carbonate formations. The abundance of monocrystalline quartz (with recycling evidence), the scarce unstable minerals (feldspars, micas), and the presence of ultra-stable heavy minerals (zircon) point to a probable multicyclic origin derived from the African Craton in tune with paleogeographic position of the basins. During the Cenozoic deposition, the analysis of provenances suggest that some areas of the West African Craton, Pan-African belt, and Variscan Moroccan Atlas were tectonized, rised, and eroded, and sedimentary rocks of the Eastern Moroccan Mesetas took place, probably because of the forebulge processes related to the Maghrebian Flysch Basin subduction.

5.5. Mineralogical evidences

The whole-rock and clay-fraction associations found in the studied lithofacies in the Intrarif, Mesorif, and Prerif sub-Domains are similar to those described in other detrital aluminic-magnesic rich Paleogene marine sediments of the proto-Mediterranean Sea and Northern Atlantic Ocean (Pletsch, 1997; Patchineelam and de Figueiredo, 2000; Alcalá et al., 2001, 2013a, 2013b; Maaté et al., 2017; Martín-Martín et al., 2022a).

The clay-mineral associations that indicate potential External Rifian source areas are relatively well-known: (i) Ill+Chl ± Kln for upper Jurassic and lower Cretaceous epicontinental formations with noticeable presence of chlorite affected by low-grade metamorphism (Azdimousa et al., 2003; El Ouahabi et al., 2014); (ii) Ill+Kln ± (I-S) + Sme and Ill+(I-S) ± Sme + Kln for Albian–Cenomanian marine formations with remarkable abundance of inherited palygorskite (up to 50 % of the clay fraction) and kaolinite (El Ouahabi et al., 2014); and (iii) Ill+Sme ± (I-S) + Kln and Ill+Sme ± (I-S) from smectite-rich upper Cretaceous and Paleogene marine formations, respectively (Faleh and Sadiki, 2002; Maaté et al., 2017; Martín-Martín et al., 2022a). The variable abundances of inherited chlorite from the late Jurassic to early Cretaceous, random mixed layer I-S, kaolinite and palygorskite from the Albian–Cenomanian, and smectite from the late Cretaceous and Paleogene allow us to deduce that there were different source areas during the Paleogene. Ternary plots for the main (end-members) whole-rock and clay-fraction mineral phases allow us to interpret how mineral assemblages in the studied logs (Fig. 8) have evolved from the Paleocene to the Oligocene. These clay-mineral associations are considered mixtures of mineral assemblages supplied from Jurassic to Paleogene suites. The variation of these mixtures from bottom to top of the successions attended to shifting sources over time.

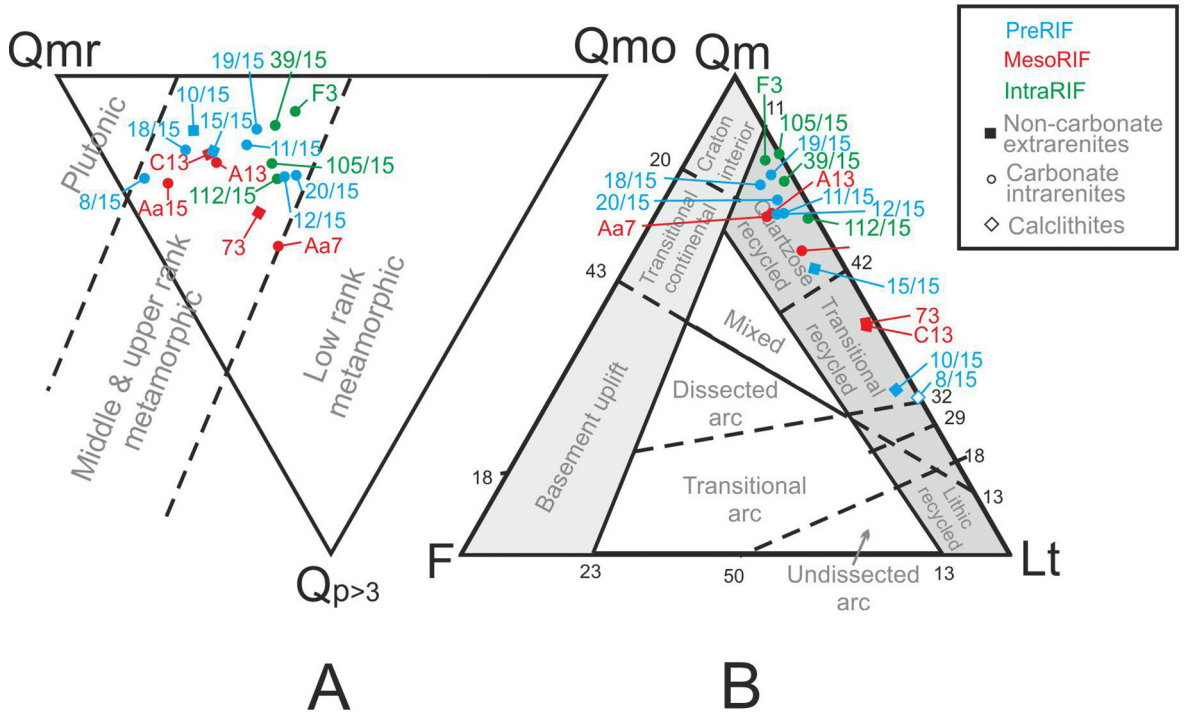

Fig. 7. Sandstone provenance diagrams from Intrarif (Logs 9, 11, 12 and 14), Mesorif (Logs 16, 17 and 19), and Prerif (Log 20) sub-Domains. (A) Qmr–Qmo–Qp ternary diagram (Basu et al., 1975; Tortosa et al., 1991); Qmr—monocrystalline quartz, undulosity <5°; Qmo—monocrystalline quartz, undulosity >5°; and Qp—polycrystalline quartz. (B) Qm–F–Lt ternary discrimination diagram (Dickinson et al., 1983); Qm—monocrystalline quartz; F—feldspars (plagioclase and K-feldspars); Lt—lithic fragments (including carbonate extrabasinal clasts [CE]). The detailed petrographic results are in the Supplementary Material A4.

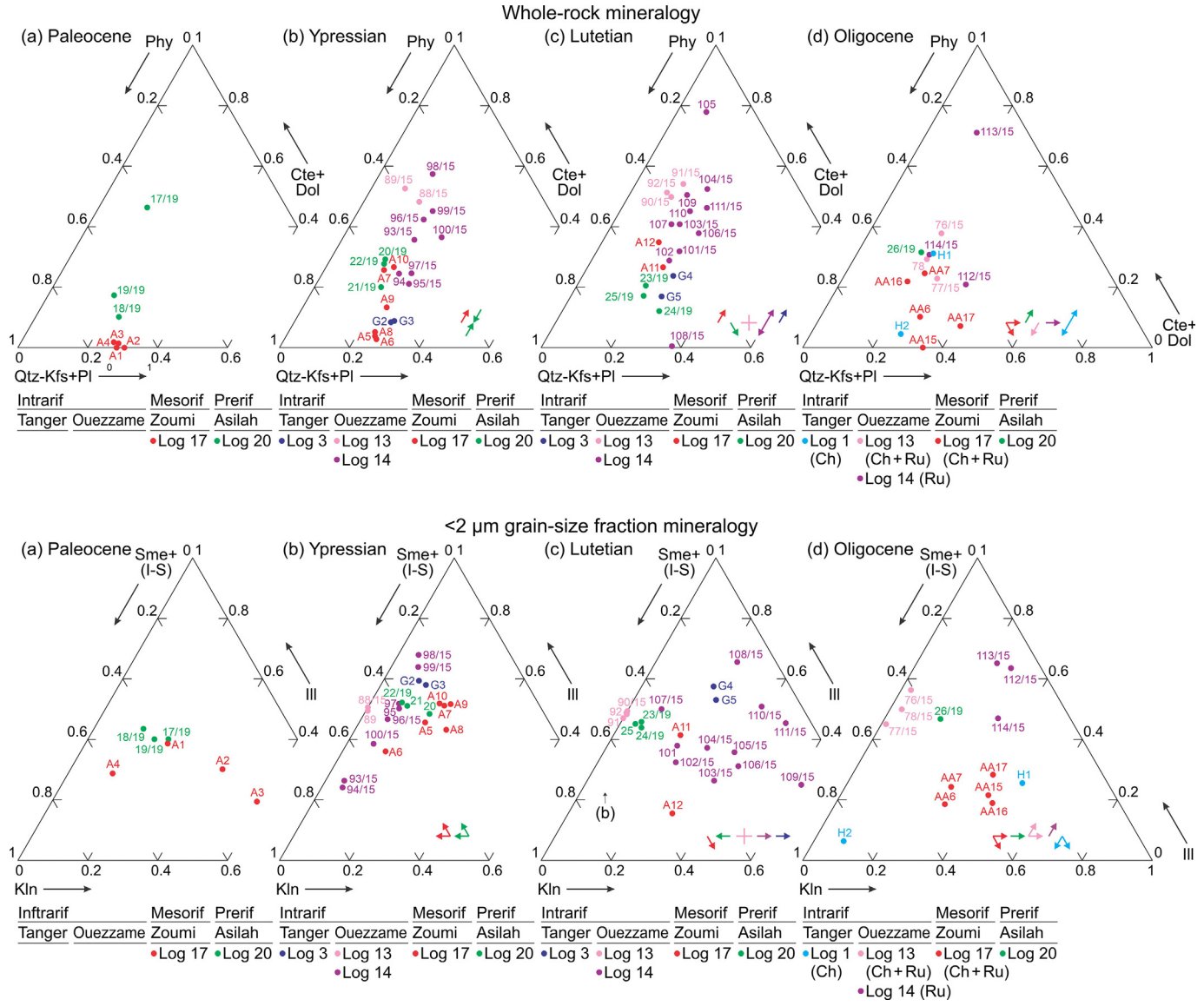

Fig. 8. Ternary plots showing the whole-rock and clay-fraction mineralogical associations from Log 1 (Saf Hamam, cian color) and Log 3 (Dear Sidi Abdallah, dark blue color) in the Tanger Sector, Log 13 (Sidi Ameur, pink color) and Log 14 (Douar Ahel Chane, purple color) in the Ouezzane Sector, Log 17 (Fej el Hanout, red color) in the Zoumi Sector, and Log 20 (Sidi M'raït, green color) in the Asilah Sector. Data are clustered by ages of sequences in each log as (a) Ypresian, (b) Lutetian, and (c) Oligocene (Fig. 2). The sample number (Fig. 2) is over the data points. Qtz—quartz; Phy—phyllosilicates; Cte—calcite; Dol—dolomite; Kfs—K-feldspar; Pl—plagioclase; Sme—smectite; Ill—illite; I-S—mixed layer illite–smectite; Kln—kaolinite. In plots (b) to (d), arrows show the evolution of the mineral assemblage of the plotted succession compared to the previous plotted succession. The detailed mineralogical results are in the Supplementary Material A5.

Regarding the source areas in the Intrarif sub-Domain, in the Tanger Sector the Ill+Kln + (I-S) ± Sme + Chl clay-mineral association identified in Ypresian and Lutetian lithofacies (Log 3), and in Chattian lithofacies (Log 1; sample H1/16) suggests a mixture of sediments mostly derived from the erosion of upper Jurassic to Albian–Cenomanian suites. Instead, the Sme + (I-S) ± Ill+Kln clay-mineral association identified in upper Chattian lithofacies (Log 1; sample H2/16) seems to be mostly derived from upper Cretaceous and Paleogene marine formations. In the Ouezzane Sector, the Ill+Sme + (I-S) clay-mineral association identified in Ypresian to Chattian lithofacies (Log 8) suggests a mixture of sediments resulting from the erosion of upper Cretaceous and Paleogene rocks. In Log 14, the Ill+(I-S) ± Sme + Kln clay-mineral association identified in Ypresian lithofacies suggests a mixture of sediments resulting from the erosion of upper Cretaceous and Albian–Cenomanian suites, whereas the Ill+Kln ± (I-S) + Sme + Chl clay-mineral association identified in Lutetian, Rupelian, and Chattian lithofacies is interpreted to be derived from a mixture of deposits from upper Jurassic to Paleogene rocks.

In the Mesorif sub-Domain, the Ill+(I-S) ± Sme + Kln clay-mineral association identified in Paleocene to Chattian lithofacies in the Zoumi Sector (Log 17) suggests a mixture of deposits from upper Cretaceous and Albian–Cenomanian successions.

Regarding the source areas in the Prerif sub-Domain, in the Asilah Sector the Ill+(I-S) ± Sme + Kln clay-mineral association identified in Paleocene and Ypresian lithofacies (Log 20) seems to be derived from a mixture of sediments from upper Cretaceous and Albian–Cenomanian rocks. The Ill+(I-S) ± Sme + Kln + Chl clay-mineral association in Lutetian and Rupelian lithofacies suggests a mixture of deposits from upper Jurassic to Paleogene deposits.

In spite that the ubiquitous presence of illite, smectite and kaolinite may limit more fine interpretations, their relative abundances together the presence of chlorite, palygorskite and certain whole-rock mineral phases enables to discriminate different source areas, as well as to propose a source-area history marked by a complex erosional evolution. The absence of a clear unroofing trend very probably indicates a sedimentary supply from different source areas eroding cohetaneously at

different rate, thus resulting into a mixture of different lithotypes dating back to upper Jurassic.

However, the above described ubiquitous presence of illite, smectite and kaolinite identified in all the studied successions becomes an advantage to use the S + K:I ratio changes (Daoudi et al., 1995; Alcalá et al., 2013a, 2013b) as a proxy of relative proximity of the source area feeding each succession over time. With the purpose to minimize misleading interpretations, X-ray parameters were used to recognize possible tectonic influences overprinting inherited mineralogy, and certain whole-rock and clay-fraction mineral phases were of assistance to identify specific sedimentation conditions. These additional criteria were used to segregate the above described clay-mineral assemblages, especially those smectite-rich derived from upper Cretaceous and Paleogene rocks.

Considering that different source areas with similar mineralogy (ubiquitous presence of illite, smectite and kaolinite) produce the mixture of sediments that feeds each succession over time, the higher S + K:I ratios in the Zoumi Sector (Mesorif sub-Domain) compared to the Asilah Sector (Prerif sub-Domain) (Fig. 4) suggest more distal and deep supplies in the first one during the Paleocene, as corroborated by the absence of calcite. This feature suggests supplies from near source areas, probably emerged sectors of the Intrarif sub-Domain. During the Ypresian, the (S + K):I ratios (Fig. 4) indicate the greater distality or minor terrigenous supply in the Zoumi Sector (Mesorif sub-Domain). During the Lutetian, the (S + K):I ratios (Fig. 4) indicate similar conditions of distality or terrigenous supply than in the Ypresian successions. During the Oligocene, a greater supply and reworking probably related to tectonics in both sectors are inferred, as corroborated by the increasing amount of quartz and illite, the decreasing amount of smectite, and the presence of chlorite (Logs 1, 3, 14 and 20). This is interpreted as a proximal supply (slope), which is also corroborated by the lowest (S + K):I ratios. During the Rupelian (Fig. 4), the (S + K):I ratio indicates a higher distality and depth in the Ouezzane Sector (Intrarif sub-Domain). During the Chattian (Fig. 4), the (S + K):I ratio increases markedly in the Tanger Sector (Intrarif sub-Domain) and Zoumi Sector (Mesorif sub-Domain), probably indicating a strong reworking of smectite- (from upper Cretaceous and Paleogene deposits) and kaolinite-rich materials (from Albian–Cenomanian deposits) rather than a greater distality. In terms of proximality-distality for source areas, it seems that during Paleocene to Eocene the sediment supply could arrive from the Intrarif Domain, being the distalmost area the Mesorif sub-Domain. It is in good agreement with the existence of a basin branch in the Mesorif–External Intrarif area as pointed by some authors (Benzaggag, 2016; Michard et al., 2014, 2018). During the Oligocene the terrigeneous supply increases, thus indicating a tectonic reactivation of reliefs with distalmost areas in the Intrarif sub-Domain.

5.6. Thicknesses analysis

This analysis carried out in the different sectors seems to suggest the occurrence of main depocenters in the western External Rif Zone, and therefore of possible basement tectonic movements (Fig. 9). Although no corrections have been made for sediment compaction, the analysis provides some insights about relative thicknesses, so allowing comparisons between different sectors. This evaluation was carried out for the whole Paleogene successions (Fig. 9A), and also separately for the Ypresian–Lutetian (Fig. 9B) and Oligocene (Fig. 9C) deposits, which in our opinion after their deposition may have been affected to a lesser extent both by tectonic lamination and erosion.

5.6.1. Paleogene thicknesses

For the entire Paleogene (Fig. 9A) the greatest thicknesses are located in the Ouezzane Unit (External Intrarif), and especially in the Mesorif and Prerif. However, the Miocene sediments are practically absent in the innermost units. Only the Tanger Unit (Internal Intrarif) checked in Log 1, and to a much lesser extent the Loukkos Unit (Internal Intrarif; Log 6) show a lower Miocene succession, even if the latter is of uncertain dating. Therefore, it cannot be ruled out that a recent erosion may have eliminated part of the originary succession.

As regards with the thickert and most complete units, it is worth highlighting the thickness of about 2.500 m of the Zoumi Unit (Internal Mesorif; Log 17). Also, the Larache Unit (Internal Prerif; Log 21) and the Ouezzane Unit (External Intrarif; Log 14) show important thicknesses higher than 1500 m and 1000 m, respectively. The Taounate Unit (External Mesorif; Log 19), and Ouezzane Unit (External Intrarif; Log 15) have thicknesses quite similar and slightly >700 m.

To avoid as much as possible any loss thickness due to erosion and/or tectonics, the analysis has been addressed to specific stratigraphic intervals. The first and most reliable one is the Ypresian–Lutetian interval (Fig. 9B), since the Paleocene is not always present, due to a depositional hiatus. Also, the Bartonian-Priabonian interval is usually missing, due to erosion caused by the unconformity at the Eocene–Oligocene boundary. The Ypresian–Lutetian interval is usually not affected by these problems and therefore is represented in almost all outcrops analyzed.

5.6.2. Ypresian–Lutetian thicknesses

Likewise to the entire Paleogene, the maximum thicknesses of this interval are recognizable in the Ouezzane Unit (External Intrarif) the Mesorif and Internal Prerif. Equaly to the Cenozoic, the thickest successions are as follows: 1500-m-thick Zoumi Unit (Internal Mesorif; Log 17), >1000-m-thick Larache Unit (Internal Prerif; Log 21), and about 300-m-thick Ouezzane Unit (External Intrarif; Log 14) and Taounate Unit (External Mesorif; Log 19). As for synsedimentary tectonics, the Ouezzane Unit (External Intrarif) and especially the Internal Mesorif and Internal Prerif could be proposed as the most subsiding zones during the Ypresian–Lutetian. These sub-Domains would have experienced basement deformation, resulting in a synclinorium-like area. Instead, the Internal Intrarif sub-Domain (excluding the Ouezzane Unit) would have been affected by slight and rather homogeneous subsidence, yielding thicknesses lower than 100 m in all sections.

5.6.3. Oligocene thicknesses

During the Oligocene, a homogenization of thicknesses has been constated (Fig. 9C) with mean values close to 200-m-thick. The thickest Oligocene successions are represented by the 400-m-thick Taounate Unit (External Mesorif; Log 19) and the 350-m-thick Loukkos Unit (Internal Intrarif; Log 8). During Ypresian–Lutetian these successions experienced slight subsidence, which could indicate subsidence inversion regarding the previous period and migration of depocenters.

Considering the External Rif Zone in terms of a foreland system, during the Eocene the foredeep area would correspond to the Mesorif and Prerif sub-Domains. This foredeep would be constituted by a complex of two sub-geosynclines separated by a relative bulge located in the External Mesorif. The Intrarif could represent the relative orogenic front (pushed by the Internal Rifian Zone). The Ridges Domain acted as the forebulge, while the Gharb Basin was the backbulge of the system. During the Oligocene, the depocentral area migrated southward and a certain homogeneization of thicknesess and sedimentation rate is constated in the whole External Rif Zone. In this new configuration, the foredeep would be located in the External Mesorif (formerly a relative bulge) while the Ridges Domain continued to act as the forebulge and the Gharb Basin as the backbulge of the system.

6. Paleogeographic and plate-tectonic evolution

On the basis of previous regional analysis, this section proposes a tentative 2D evolutionary model of the External Rif Zone during the Cenozoic (Fig. 10). The paleogeographic maps of this Figure are based on paleo-tectonic reconstructions of the area from Le Breton et al. (2021) and Müller et al. (2019). The paleo-coastlines and the paleoplate boundaries were extracted for two time steps, 70 Ma (Fig. 10A)

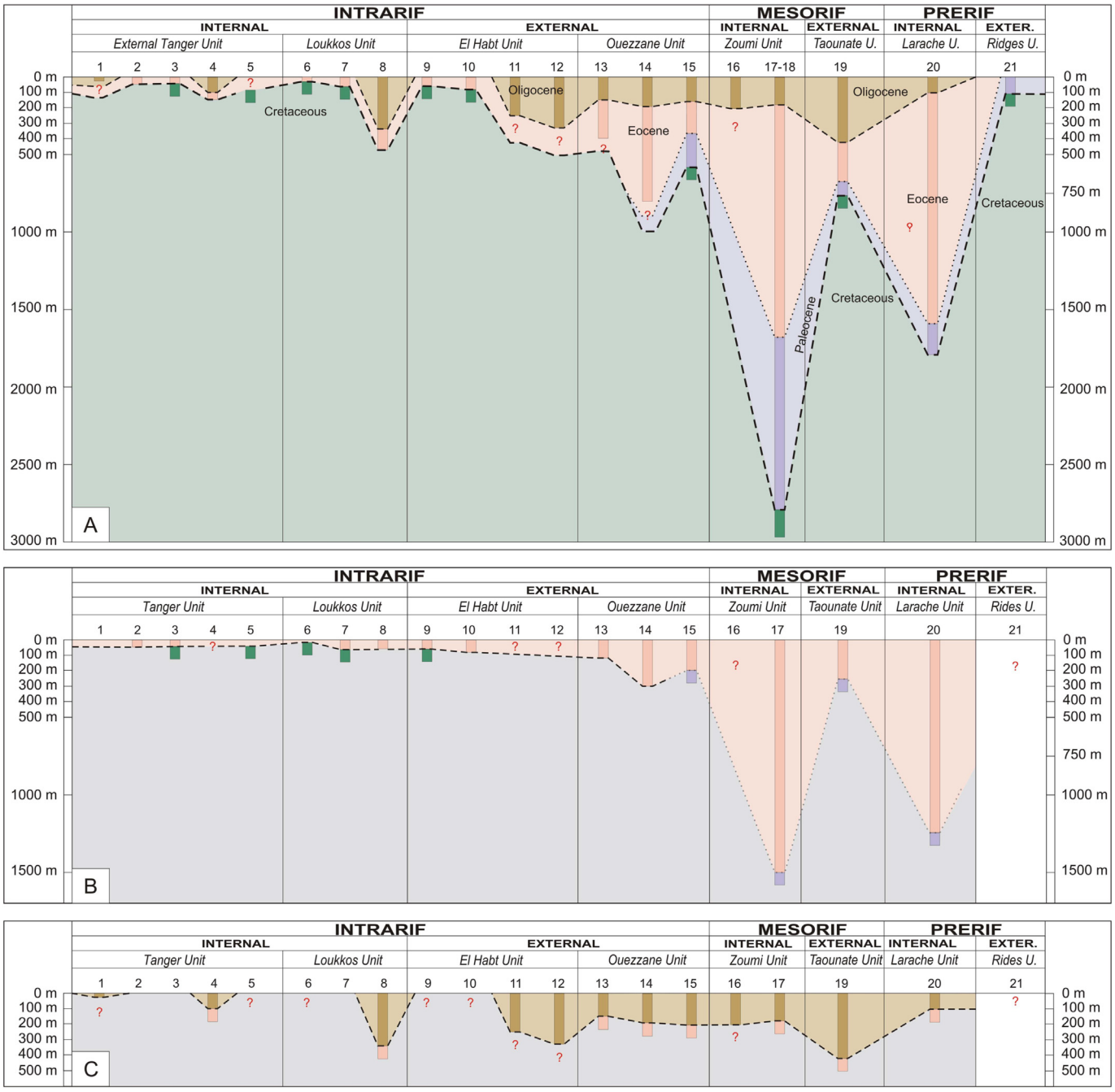

Fig. 9. Subsidence analysis of the External Rif Zone area. (A) Paleogene subsidence; (B) Ypresian–Lutetian subsidence; (C) Oligocene subsidence.

and 40 Ma (Fig. 10B), relative to Europe fixed, using the software GPlates (Müller et al., 2018).

Fig. 10A and lower section from Fig. 10C show how the maximum expansion of the North African Margin was reached during the Cretaceous after a long extensional phase that began in the Triassic. During this phase we assume the presence of an ocean (Maghrebian Flysch Basin) located between the Mesomediterranean Microplate and the North African Margin, which is in turn subdivided into different domains and subdomains according to their paleogeographic location source areas, and tectonic context. The whole North African Margin–Maghrebian Flysch Basin system included minor lateral branches of oceanic-transitional crust as attested by the presence of mafic rocks in the External Rif Zone (Benzaggag, 2016). However, Michard et al. (2018) consider this magmatism as a manifestation of the Central Atlantic Magmatic Province activity. This interpretation is based on the U—Pb zircon dating at 190 ± 2 Ma of one gabbro of the Mesorif Subzone (External Rif Zone), which appears to be coeval with the early opening of the Central Atlantic occurring before the opening of the Maghrebian Tethys. The tectonic style observed in the Ouezzane and El Habt Unit is characterized by unrooted floating and extruded nappes and is different with respect to the other external units, which are characterized by a minor tectonic shortening. In our opinion, unrooted-extruded nappes is the typical tectonic style produced in accretionary prims in front of subduction zones (similarly to the Maghrebian Flysch Basin units). Therefore, this last reconstruction supports the occurrence of a lateral oceanic branch with oceanic-transitional crust corresponding to the External Intrarif.

In the latest Cretaceous, the tectonic inversion took place with the transition from an extensional to a compressional tectonic regime, as well documented in literature (Stampfli et al., 2002). During the

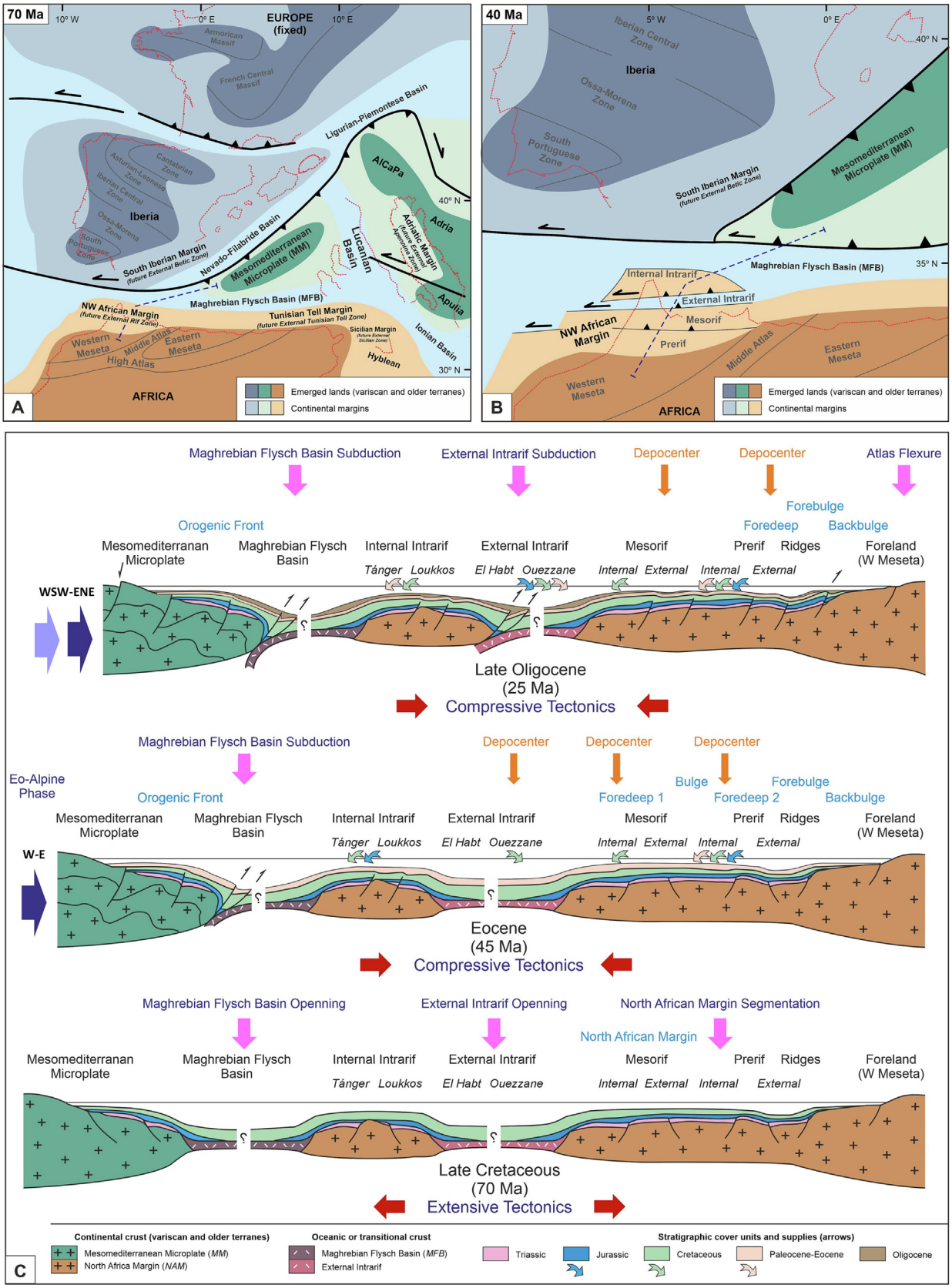

Fig. 10. Paleogeographic–tectonic evolution based on plate tectonic reconstructions of Müller et al. (2019) and Le Breton et al. (2021). (A) Overall paleogeographic–tectonic map of the western–central Mediterranean area at the late Cretaceous times; (B) Detailed paleogeographic–tectonic map of the External Rif Zone area at the middle Eocene times; (C) Detailed paleogeographic tectonic cross-sections of the External Rif Zone area with evidences of the crustal basement, and emphasizing the stratigraphic cover units at the late Cretaceous, middle Eocene, and Oligocene. These paleogeographic tectonic cross-sections incorporate information on the main regional stress (horizontal big dark-blue arrows), the areas with compressive or extensional tectonics (red horizontal arrows), the opening and subduction marine areas, extensional segmentation and compressive flexure (all marked with pink vertical arrows), the subsiding areas (depocenter marked with thin vertical orange arrows), and the position and kind of source areas in time (reclined curved arrows: Jurassic in blue, Cretaceous in green, and Paleogene in light pink).

Paleogene (Fig. 10B), the Eoalpine Phase (Alpine *s.s.*) developed also involving the northern margin of the Mesomediterranean Microplate (Guerrera et al., 2021). This compressional phase caused the closure of the Nevado-Filábride-Ligurian-Piemontese oceanic branch to form the Alps and Pyrenees, and other chain systems (Martín-Martín et al., 2001).

In the late Paleogene (Fig. 10C; middle section), the main compressive stresses would have a W–E orientation (Martín-Algarra, 1987), and the subduction of the Maghrebian Flysch Basin under the Mesomediterranean Microplate would begin at the end of this period (Guerrera et al., 2021). This process would mark the transition of the External Rif Zone to a complex foreland basin system comprising subsiding oceanic branches (or with transitional thinned crust) located in the External Intrarif and between the Intrarif and Mesorif subdomains (Benzaggag, 2016). At this time the Internal Intrarif became a relative orogenic front facing the foreland (Fig. 10B–C). The Eoalpine orogenic Phase would have generated a compressional deep-seated deformation (bulges and blind thrusts) in the External Rif Zone that would result in the complexity of the margin physiography. This is characterized by some zones with more subsidence (foredeep and backbulge areas) than other ones (relative bulge and forebulge areas) (Guerrera et al., 2021). Flexural subsidence caused increased slope and margin failure, which became tectonically active so activating olistostromes, slumps and turbidity currents. Tectonic activity reached its maximum during the Oligocene, and its results extends to the outermost sectors of the external foreland basin (Fig. 10C).

During the Paleocene-Eocene the fine terrigeneous deposits seems to indicate exhumation of older terrains as follows: Jurassic-Cretaceous in the Internal Intrarif, Cretaceous in the External Intrarif and Mesorif, a mixture of Jurassic to Paleogene in the Prerif.

In the case of the Oligocene the fine terrigeneous deposits seems to indicate exhumation also of older terrains as follows: Cretaceous-Paleogene in the Internal Intrarif, a mixture of Jurassic to Paleogene in the External Intrarif, Crataceous in the Mesorif, a again mixture of Jurassic to Paleogene in the Prerif.

Fine terrigeneous supplies are thought to derive from local rising terrains due to the Eo-Alpine tectonics due to basement folding and reversion of former normal faults into inverse blind-thrusts. Therefore, in the Internal and External Intrarif this rising domain could be located in the Loukkos area (the less subsident). In the case of Mesorif and Internal Prerif the source area could be located in the External Mesorif and/or the Ridges areas (also low subsidents).

During the whole Paleogene the medium-grained terrigenous supply (calcarenites and sublitarenites) indicate the erosion of a recycled metamorphic orogen (Hercynian or older), which probably corresponds to the Atlas Chain located in the foreland.

From the late Oligocene (Fig. 10C; upper section), the Neoalpine orogenic phase develops with a southern vergence (WSW) originating the Maghrebian Chain and its lateral extents (Betic Cordillera and Southern Apennines) (Critelli, 2018; Guerrera et al., 2021). The development of this orogeny would generate the flexure in the previous Atlas front that some authors (Khomsi et al., 2006, 2009) consider at the Oligocene–Miocene boundary. At the end of the Oligocene, the subduction onset of the Maghrebian Basin occurred (Zeck, 1996; Lonergan and White, 1997; Vissers, 2012; De Lis Mancilla et al., 2013). The related slab roll-back would have caused the beginning of the opening of the Alborán Sea as a western extent of the Algerian-Provencal Basin in a back-arc basin context due to a local extension (Zeck, 1996; Lonergan and White, 1997; Brun and Faccenna, 2008; Vergés and Fernández, 2012; Bezada et al., 2013).

7. Comparison with other Tethyan margins of the central–western Mediterranean chains

The Paleogene evolution of the studied external Rifian domains was compared to that of other external margins along the Betic-Magrebian-Apennine chains (South Iberia, Tunisian Tell, Sicily, and Apennines). The main similarities and some singularities are described below and a table with the main finding of the correlation are in the Supplementary Material A6.

7.1. South Iberian Margin, External Zones of the Betic Chain

The South Iberian Margin is nowadays represented by the External Betic Cordillera in South Spain. In the past, it was a part of a wide old alpine margin located in the westernmost Tethys (Fig. 10A). The area is classically divided from south to north into tectono-paleogeographic units separated by NW-vergent tectonic contacts (Vera, 2004): the mainly pelagic Subbetic Domain and the Prebetic neritic Domain. Concerning the Jurassic successions, the Subbetic Domain is in turn divided from S to N into internal (shallow pelagic), intermediate (deep pelagic), and external (shallow pelagic) subdomains, while the Prebetic Domain is divided into internal (neritic) and external (neritic to shallow-water) subdomains. At about the Cretaceous–Cenozoic boundary (Fig. 10A) a tectonic inversion occurred in this margin. This inversion provokes the subduction of the Nevado-Filabride Basin below the Mesomediterranean Microplate (locally internal zone of the Alpine System), successively evolving as a foreland basin (Vera, 2000; Guerrera et al., 2006, 2014). The Paleogene paleogeography is inherited from the Mesozoic history, but a deep-seated deformation caused a plate flexure, while the previous Mesozoic normal faults (horst and graben tectonics) evolved as blind thrusts. In this context, shallow pelagic zones became eroded emergent anticlines. This evolution leads to the diversification of lithofacies within deep marine basins located between the rising emergent areas and erosional gaps in the shallower areas (Fig. 11). So, in the deep Subbetic areas (mainly in the intermediate sector), *scaglia*-like lithofacies deposited (Capas Rojas and Capas Blancas fms), characterized by frequent olistostromes (Píñar Group) and turbidite deposits (Cardela Group) near the emergent reliefs more frequent in the Oligocene. On the contrary, in the external Prebetic Domain, a shallow nummulite platform (Cañada Hermosa Fm) developed, while in the internal Prebetic Domain frequent nummulite-rich turbidites (Nablanca Fm) deposited, which pass laterally to deep water varicoloured *scaglia*-like deposits. A noticeable similarity is recognized between the External Rif Zone evolution and the Subbetic evolution. In both cases, Paleogene tectonics due to the Eo-Alpine phase and related to the Nevado-Filabride Basin subduction below the Mesomediterranean Microplate is constated (Martín-Algarra, 1987). Nevertheless, this tectonics was stronger in the South Iberian Margin than in the External Rif Zone.

7.2. External Zones of the Tunisian Tell, NE African Margin

The External Zones of the Tunisian Tell correspond to a wide alpine margin (Rouvier, 1985; Wildi, 1983; Belayouni et al., 2012) classically divided from S to N into four tectono-paleogeographic units separated by S-vergent tectonic contacts: the Numidian Zone (Numidian Nappe, Col de Adissa, Aïn Drahan, and Kasseb units), the Triassic Dome Zone (Aïn El Bey Unit), the Intermediate Atlas Zone; and the Saharian Zone. This margin and the South Iberian Margin show a similar evolution. During the Mesozoic the above-mentioned Numidian and Triassic Dome zones represented deep areas, while the Atlas and Saharian zones were shallow-water areas. The Paleogene paleogeography was inherided from the passive margin Mesozoic evolution, favouring the deposition of a high variety of lithofacies and the appearing of unconformities with gaps (Fig. 11). Nummulite platform deposits characterize the El Gueria Fm, while different lithofacies of *scaglia*-like deposits with fine terrigeneous supply (El Haria and Souar fms), or calcareous *scaglia*-like (Bou Dabbous Fm) deposits characterize the Numidian and Triassic Dome zones (Belayouni et al., 2012). This margin was affected by the Eo-Alpine tectonics with the appearance of distal slump deposits in the El Haria and Souar fms (locally called 'boules jaunes'). Moreover, growth folds in the Kasseb Unit and the carbonate lithofacies of the Bou

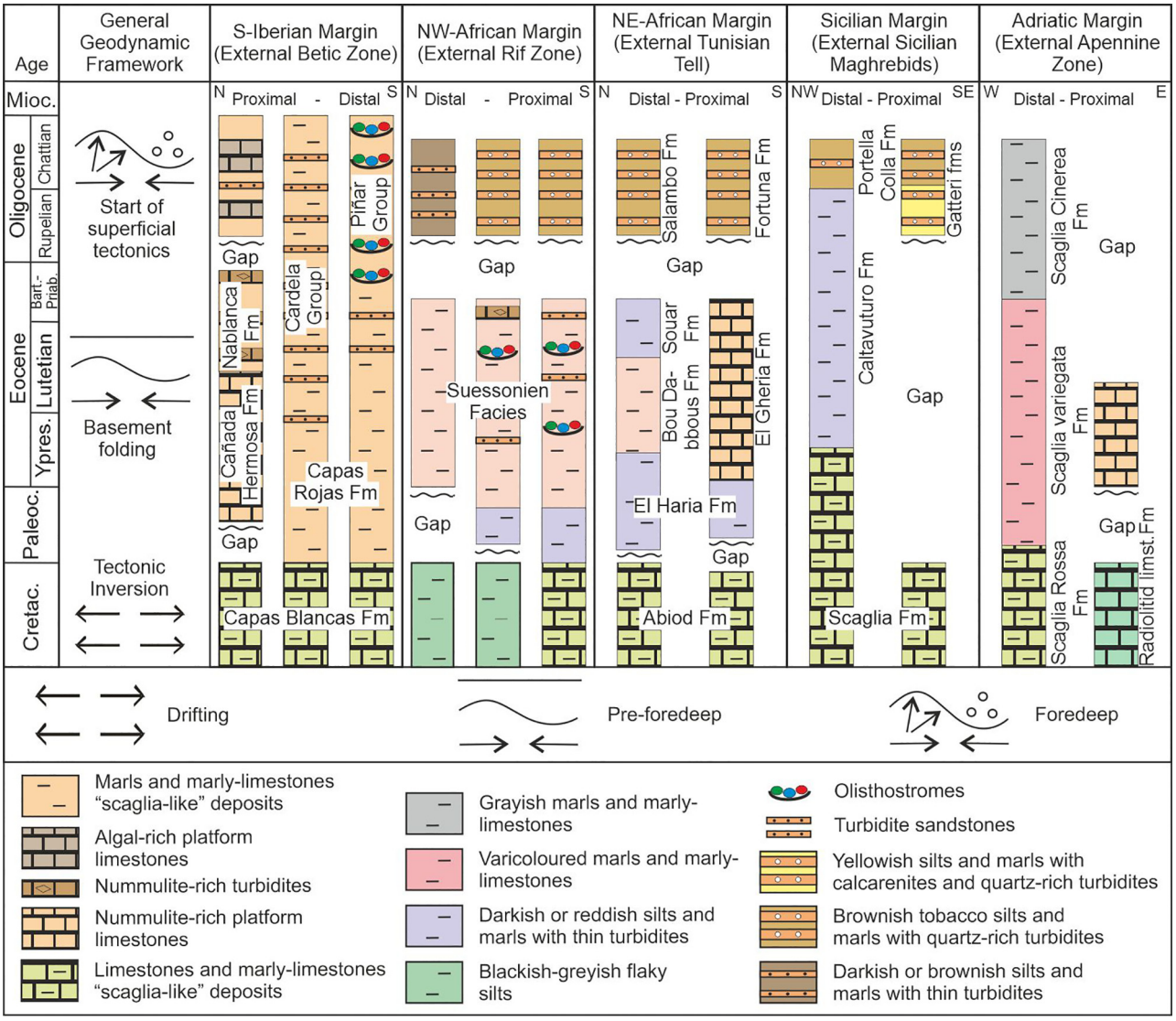

Fig. 11. Main similitude and differences in the evolution of the compared margins. A table with the main results of the correlation are in the Supplementary Material A6.

Dabbous Fm pass laterally to varicoloured marly-pelitic *scaglia*-like deposits. Oligocene deposits are made of tobacco marls and silts with quatz-rich thin turbidites from the Salambo and Fortuna Fms. In the Tunisian Tell the tectonic deformation seems to be gentler than in the External Rif Zone and the South Iberian Margin. This is probably due to the increasing distance of the Tunisian Tell from the areas affected by the Eo-Alpine tectonic activity (Internal Betic Cordillera, Pyrenees, Iberian Range, and Alps), and therefore to a minor Maghrebian Basin subduction rate below the Mesomediterranean Microplate.

7.3. External Zones of the Sicilian Maghrebids

The SE-vergent External Zones of the Sicilian Maghrebids mainly crop out in the western sector of Sicily (Madonie Mts) and show a paleogeographic and tectonic evolution similar to the previous described margins (Fig. 10A). It is widely accepted that the paleogeographic differences characterizing the external domains result into two main successions deposited in a margin-basin system: the middle Triassic–Oligocene Panormide carbonate platform succession, and the middle Triassic–Oligocene Imerese Basin deep-water succession. The latter are characterized by prevailing pelagic deposits (Sicano Basin), which pass towards east to sectors bordered by shallow water and pelagic platforms (Trapani-Saccense and Iblean Foreland). The Panormide platform Unit overrides the Imerese deep-water Unit (Henriquet et al., 2020). The Mesozoic paleogeographic setting is characterized by structural highs and basin areas (horst and graben and/or semigraben structures), where the different successions developed (Basilone and Sulli, 2018). The distribution of the Paleogene interval of the Panormide (relatively proximal), and Imerese (relatively distal), successions is controlled by the evolution of paleogeographic features inherited from the Jurassic–Cretaceous structural setting. The Paleogene tectonic deformation related to the Eo-alpine tectonics recognized in the above described external chain sectors affected also the Sicilian margin, modifying the previous depositional areas. This evolution produced more diversified Paleogene lithofacies marked by an increasing amount of terrigenous supply (coming even more from external sectors of the African Margin) and the appearing of unconformities with gaps in the proximal sub-domain (Fig. 11). In general, the main Paleogene formations are represented by varicoloured *scaglia*-like deposits. In the Gratteri Fm (Oligocene *p.p.*, Panormide Domain), which lies above an evident unconformity surface, the occasional presence of quartz-rich sandstones and calcarenites interbedded with yellow silty marls is recognizable. Some beds are rich in larger foraminifers (lepidocyclinids and nummulitids), while the planktonic foraminifers are badly preserved or absent, probably due to dissolution. Also, in the Eocene–Oligocene *p.p.* Caltavuturo Fm (Imerese Domain), badly preserved hyaline benthic agglutinated or planktonic foraminifera are

present, while larger foraminifers (nummulitids) are common especially within thin resedimented breccia beds. The occurrence of synsedimentary faults and folds at different stratigraphic levels of the Paleogene successions completes the similarity with the external sectors previously considered.

As regards the unconformable boundaries and stratigraphic gaps identified in the Rifian successions (see above), and those pointed out in the other sectors (e.g. Panormide and Imerese units) it is difficult to establish precise lateral correlations. This is mainly due to the difficulty of recognizing similar unconfomities and related gaps.

7.4. External Zones of the Apennine Chain, Adriatic Margin

The E-vergent External Zones of the Apennines are represented by two sectors belonging to the Adria Margin located north and south of the Ancona-Anzio tectonic line: the more external northern Umbria-Marche Domain (distal) and the more internal southern Lazio-Abruzzi (proximal), and the Campania-Lucania Domain. Even if these areas show some paleogeographic peculiarities, the general evolution is comparable with the previously considered chain sectors of the South Iberian and African margins (Fig. 10A).

The Umbria-Marche, Lazio-Abruzzi, and Campania-Lucania units are represented by sedimentary successions deposited on the Hercynian continental crust of the Adria-Africa Margin, dismembered and drifting northward during the Cenozoic to reach the present position. The Alpine history of these units started about 200 Ma ago, when the previous Hercynian orogen was affected by marked extensional tectonics causing progressive rifting, which led to the development of the passive Adriatic Margin. This extension generated horst and graben structures and caused a sedimentary differentiation due to the presence of pelagic basin areas separated by structural highs.

The Paleogene lithofacies are influenced by the early change of the tectonic regime from extension to compression, and differ from the older deposits because of an increase of the terrigenous supply and by the appearing of unconformities in the proximal sub-domain (Fig. 11). In the Umbria-Marche area the representative formations are constituted by varicoloured *scaglia*-like deposits (Scaglia Rossa *p.p.*, Scaglia Variegata and Scaglia Cinerea fms; Guerrera et al., 1989; Pantaloni et al., 2016; among others), which show consistent lateral thickness variations and are marked by the occurrence of *syn*-sedimentary deposits such as (mainly Paleocene) carbonate turbidite beds, slumps and olistostromes (tectofacies) with different thicknesses and at different stratigraphic levels. Moreover, lateral lithofacies changes are recognizable, and synsedimentary faults and (probably) minor folds are observable. The passage to the Miocene is characterized by the presence of volcaniclastic levels as the Raffaello marker bed (Guerrera et al., 2015). This general evolution indicates an upward increasing tectonic activity. Similar Paleogene lithological suites and synsedimentary structures are also recognizable in the Lazio-Abruzzi and Campania-Lucania domains. In particular, the Lazio-Abruzzi platform domain shows an unconformity between lower (Peritidal limestones) and upper Cretaceous (Radiolitid Limestones Fm) and a second unconformity causing a gap up to lower Eocene (scattered limestone beds; Tomassetti et al., 2016; among others). After a further gap the succession resumes with lower-middle Miocene deposits (Lithothamnion and Bryozoan Limestones; Brandano, 2017).

7.5. Synthesis of this comparison

The comparision of the Paleogene evolution between different external margins of the Iberia-Africa-Adria plates reveals important similarities and few differences. The vergence of the units of each sector is different from margin to margin (S-SW for Rif and Tell; SE for Sicily; E-NE Apennine; while for the Betides is NW), always directed towards the foreland. However, while the Betics show an alpine vergence, in the other cases it is Apennine-Maghrebide type. The selected formations are representative of each considered margin being partially different but showing a similar palaeogeographic and tectonic evolution (Fig. 11). The Eo-Alpine tectonics is recognized everywhere but it seems to decrease from N to S and from W to E in the Western Tethyan domains. In all cases, this Paleogene tectonics is mainly related to the subduction of a northern oceanic Tethyan branch (Nevado-Filabride and Liguria-Piemontese basins) below the Mesomediterranean Microplate (Fig. 10A), which represented the Internal Zones of the chain. In all the cases, the most deformed areas were the Internal Zones more affected by the Eo-Alpine tectonics (NW vergence). During the tectonic inversion (Latest Cretaceous), the margins of the different plates started to behave as foreland basins due to the subduction of the Tethyan oceanic branches. In the sedimentary records of the compared margins, two unconformities with associate gaps are recognized in the shallow (proximal) sub-domains in comparable periods (Cretaceous-Cenozoic and Eocene-Oligocene boundaries). The pre-foredeep phase took place during the Paleocene-Eocene (after the first unconformity) with basement deformation affecting and conditioning the sedimentation in the occurrence of unconformity causing a difersification of the lithofacies. During Oligocene times (after the second unconformity) the foredeep phase started with the rising reliefs related to pellicular tectonics. This leads to the increasing of terrigenous supplies and tectonic instability in the sedimentary realms.

8. Conclusions

On the basis of a multidisciplinary methodology, this paper presents a basin analysis of the western External Rif Zone during the Paleogene. The Paleogene stratigraphic record is affected by three main unconformity surfaces coarsely aligned with the Cretaceous–Paleogene, Eocene–Oligocene, and Oligocene–Miocene boundaries. The oldest two unconformities were recognized in all the examined sectors. For this reason, they are considered principal unconformities. The youngest unconformity is less extended, and therefore is considered as a second-order one. Six main concluding remarks are listed below.

1. The Cretaceous–Paleogene unconformity is related to the tectonic inversion from extension to compression that affected the alpine Tethys domains, linked to the opening of the South Atlantic Ocean. Instead, the Oligocene–Miocene unconformity seems to be generated by a local flexural deformation phase, which affected the Atlas front. The Eocene–Oligocene unconformity, together with the evidences of Paleogene tectonics would represent side-effects of the so-called Eo-alpine orogenic phase, linked to the closure of the northern branch of the western Tethys. These three unconformities allow dividing the Paleogene stratigraphic record into two main stratigraphic units referable to the Paleocene–Eocene and Oligocene, respectively.
2. The recorded turbidites, slumps, olistostromes, and synsedimentary folds and faults are indicators of synsedimentary tectonics. These features start from late Ypresian and become very frequent during the Oligocene, so indicating an increasing upward of the synsedimentary tectonic activity.
3. The petrographic study of the Paleogene detrital suites indicate that quartz supply derives from the erosion of metamorphic rocks. All samples analyzed fall into the 'recycled orogen' tectonic setting, specifically the hybrid arenites and calcilithites field, which corresponds to the 'transitional recycled' sub-type. Most of terrigenous extrarenites belong to the middle–upper metamorphic rank, very probably derived from the Atlas Chain and/or the African Craton.
4. The mineralogical study of the Paleogene mudstone suites evidences a complex erosional evolution. The source-area history reconstructed in the studied area indicates that the source areas during the Paleocene–Eocene could be located in the Internal Intrarif, the distalmost area being the Prerif, and that the provenance reverses during the Oligocene. The absence of a clear unroofing trend

probably indicates a multi-source area with sediments from different rock-suites of different ages mixing in variable proportions over time.

5. The subsidence analysis indicates that considering the External Rif Zone in terms of a foreland basin, during the Eocene the foredeep area would correspond to the Mesorif and Prerif sub-domains. The configuration of this foredeep would be characterized by a complex formed by two 'sub-geosynclines', separated by a relative bulge located in the External Mesorif. In this framework, the Internal Intrarif could represent the advancing relative orogenic front. The Eocene forebulge area would correspond to the Ridges Domain, while the Gharb Basin was the backbulge area of the system. During the Oligocene the depocentral area migrates southward, accomplishing a subsidence homogenization in the whole External Rif Zone. In this new configuration, the foredeep would be located in the External Mesorif (previously a relative bulge) while the Ridges Domain and the Gharb Basin continued to act as the forebulge and the backbulge of the system, respectively.
6. The comparision with the Paleogene evolution of different external margins of the central–westen Mediterranean chains reveals important similarities and few differences. All the correlated zones are characterized by different tectono-paleogeographic units with a vergent towards their respective forelands. This deformation is substantially contemporaneous in the case of the Eo-Alpine tectonics but its effects on the sedimentation decrease from N to S and from W to E in the Western Tethyan domains as we move away from the Eo-Alpine deformational focus. The Paleogene evolution of the foreland basins in the compared margins shows equivalent unconformity surfaces and gaps separating the pre-foredeep (Paleocene-Eocene) and the beginning of foredeep (Oligocene) stages, respectively.

Supplementary data to this article can be found online at https://doi.org/10.1016/j.sedgeo.2023.106367.

Data availability

Data will be made available on request.

Declaration of competing interest

Manuel Martín-Martín on behalf of all authors declare no conflict of interest. Also, the Funding are here mentioned: PID2020-114381GB-I00 research project (Spanish Ministry of Education and Science).

Acknowledgments

Research supported by PID2020-114381GB-I00 research project (Spanish Ministry of Education and Science), Research Groups and projects of the Generalitat Valenciana from Alicante University (CTMA-IGA). The contribution of two anonymous reviewers is acknowledged.

References

Abbassi, A., Cipollari, P., Zaghloul, M.N., Cosentino, D., 2021. The Numidian Sandstones in northern Morocco: evidence for early Burdigalian autochthonous deposition on top of the Tanger Unit. Marine and Petroleum Geology https://doi.org/10.1016/j.marpetgeo.2021.105149.

AitBrahim, L., Chotin, p., Hinaj, S., Abdelouafi, A., El Adraoui, A., Nakcha, Ch., Dhont, D., Charroud, M., SosseyAlaoui, F., Amrhar, M., Bouaza, A., Tabyaoui, H., Chaouni, A., 2002. Paleostress evolution in the Moroccan African margin from Triassic to Present. Tectonophysics 357, 187–205.

Alcalá, F.J., Martín-Martín, M., López-Galindo, A., 2001. Clay mineralogy of the Tertiary sediments in the Internal Subbetic of Málaga Province, S Spain: implications for geodynamic evolution. Clay Minerals 36, 615–620.

Alcalá, F.J., López-Galindo, A., Martín-Martín, M., 2013a. Clay mineralogy as a tool for integrated sequence stratigraphic and palaeogeographic reconstructions: Late Oligocene-Early Aquitanian Western Internal South Iberian Margin, Spain. Geological Jounal 48, 363–375.

Alcalá, F.J., Guerrera, F., Martín-Martín, M., Raffaelli, G., Serrano, F., 2013b. Geodynamic implications derived from Numidian-like distal turbidites deposited along the Internal-External Domain Boundary of the Betic Cordillera (S, Spain). Terra Nova 25, 119–129.

Azdimousa, A., Bourgois, J., Asebriy, L., Poupeau, G., Montigny, R., 2003. Histoire thermique et surrection du Rif externe et des nappes de flyschs associées (Nord Maroc). Travaux Institut Scientif. Univ. Mohammed V. Série Géologie et Géographique Physique 21, 15–26.

Azdimousa, A., Jabaloy, A., Asebriy, L., Booth-Rea, G., González-Lodeiro, F., Bourgois, J., 2007. Lithostratigraphy and structure of the Temsamane Unit (Eastern External Rif, Morocco). Revista de la Sociedad Geológica de España 20, 119–132.

Basilone, L., Sulli, A., 2018. Basin analysis in the Southern Tethyan margin: Facies sequences, stratal pattern and subsidence history highlight extension-to-inversion processes in the cretaceous Panormide carbonate platform (NW Sicily). Sedimentary Geology 363, 235–251.

Basu, A., Young, S.W., Suttner, L.J., James, W.C., Mack, G.H., 1975. Re-evaluation of the use of undulatory extinction and polycrystallinity in detrital quartz for provenance interpretation. Journal of Sedimentary Research 45 (4), 873–882.

Belayouni, H., Guerrera, F., Martín-Martín, M., Serrano, F., 2012. Stratigraphic update of the Cenozoic Sub-Numidian formations of the Tunisian Tell (North Africa): tectonic/sedimentary evolution and correlations along the Maghrebian Chain. Journal of African Earth Sciences 64, 48–64.

Benzaggag, M., 2016. Tholeitic basalts and ophiolitic complexes of the Mesorif Zone (External Rif, Morocco) at the Jurassic-cretaceous boundary and the importance of the Ouerrha Accident in the palaeogeographic and geodynamic evolution of the Rif Mountains. Boletín Geológico y Minero 127, 389–406.

Berggren, W.A., Pearson, P.P., 2005. A revised tropical to subtropical planktonic foraminiferal zonation of the Eocene and Oligocene. Journal of Foraminiferal Research 35, 279–298.

Berggren, W.A., Pearson, P.N., 2006. Tropical and subtropical planktonic foraminiferal zonation of the Eocene and Oligocene. In: Pearson, P.N., Olsson, R.K., Huber, B.T., Hemleben, C., Berggren, W.A. (Eds.), Atlas of Eocene Planktonic Foraminifera. Cushman Foundation Special Publicationvol. 41. Alen Press, Lawrence (Kansas, USA), pp. 29–40.

Berggren, W.A., Kent, D.V., Swisher, C.C., Aubry, M.-P., Berggren, W.A., et al., 1995. A revised Cenozoic geochronology and chronostratigraphy. Geochronology, time-scales, and global stratigraphic correlation. SEPM (Society for Sedimentary Geology), Special Publication54, pp. 129–212.

Bezada, M.J., Humphreys, E.D., Toomey, D.R., Harnafi, M., Dávila, J.M., Gallart, J., 2013. Evidence for slab rollback in westernmost Mediterranean from improved upper mantle imaging. Earth Planetary Science Letters 368, 51–60.

Biscaye, P.E., 1965. Mineralogy and sedimentation of recent deep sea clay in the Atlantic Ocean and adjacent seas and oceans. Geological Society American Bulletin 76, 803–832.

Blow, W.H., 1969. Late middle Eocene to recent planktonic foraminiferal biostratigraphy. In: Bronniman, P., Renz, H.H. (Eds.), Proceedings of the 1st International Conference on Planktonic Microfossils. Geneva (Swiss)vol. 19671, pp. 199–422.

Boukaoud, E.H., Godard, G., Chabou, M.C., Bouftouha, Y., Doukkari, S., 2021. Petrology and geochemistry of the Texenna ophiolites, northeastern Algeria: Implications for the Maghrebian flysch suture zone. Lithos https://doi.org/10.1016/j.lithos.2021.1060190024-4937.

Brandano, M., 2017. Unravelling the origin of a Paleogene unconformity in the Latium-Abruzzi carbonate succession: a shaved platform. Paleogeography, Paleoclimatology, Paleoecology 485, 687–696.

Brun, J.P., Faccenna, C., 2008. Exhumation of high-pressure rocks driven by slab rollback. Earth Planetary Science Letters 272, 1–7.

Chalouan, A., Galindo-Zaldívar, J., Akil, M., Marín, C., Chabli, A., Ruano, P., Bargach, K., Sanz de Galdeano, C., Benmakhlouf, M., Ahmamou, M., Gourari, L., 2006. Tectonic wedge expulsion in the southwestern front of the Rif Cordillera (Morocco). In: Moratti, G., Chalouan, A. (Eds.), Tectonics of the Western Mediterranean and North Africa. Geological Society of London, special publication262, pp. 101–118.

Chalouan, A., Michard, A., El Kadiri, K.H., de Frizon Lamotte, D., Soto, J.I., Saddiqi, O., 2008. Continental Evolution: The Geology of Morocco. Lecture Notes in Earth Sciencesvol. 116. Springer-Verlag, Berlin Heidelberg (Berlin) (424 pp.).

Clark, P.U., Dyke, A.S., Shakun, J.D., Carlson, A.E., Clark, J., Wohlfarth, B., Mitrovica, J.X., Hostetler, S.W., McCabe, A.M., 2009. The last Glacial Maximum. Science 325, 710–714.

Critelli, S., 2018. Provenance of Mesozoic to Cenozoic Circum-Mediterranean sandstones in relation to tectonic setting. Earth-Science Rewiev 185, 624–648.

Critelli, S., Muto, F., Perri, F., Tripodi, V., 2017. Interpreting provenance relations from sandstone detrital modes, southern Italy foreland region: stratigraphic record of the Miocene tectonic evolution. Marine and Petroleum Geology 87, 2–14.

Croudace, J.W., Robinson, N.D., 1983. A simple, rapid and precise smear method for the preparation of oriented clay mounts. Clay Minerals 18, 337–340.

Daoudi, L., Deconinck, J.F., Witan, O., Rey, J., 1995. Impact des variations du niveaumarin sur les argiles: exemple du Crétacé inférieur du basin d'Essaouira (Maroc). Comptes Rendus de l'Académie des Sciences, Paris 320, 707–711.

de Frizon Lamotte, D., Zaghloul, M.N., Faouziya, H., Mohn, G., Leprêtre, R., Gimeno-Vives, O., Atouabat, A., El Mourabet, M., Abass, A., 2017. Rif externe: comment comprendre et expliquer le chaos apparent? Géologues 194, 13–15.

De Lis Mancilla, F., Stich, D., Berrocoso, M., Martín, R., Morales, J., Fernandez-Ros, A., Páez, R., Pérez-Peña, A., 2013. Delamination in the Betic Range: deep structure, seismicity, and GPS motion. Geology 41, 307–310.

Di Stefano, A., Foresi, L.M., Lirer, F., Iaccarino, S.M., Turco, E., Amore, F.O., Morabito, S., Salvatorini, G., Mazzei, R., Abdul Aziz, H., 2008. Calcareous plankton high resolution bio-magnetostratigraphy for the Langhian of the Mediterranean area. Rivista Italiana di Paleontologia e Stratigrafia 114, 51–76.

Dickinson, W.R., 1970. Interpreting detrital modes of graywacke and arkose. Journal of Sedimentary Research 40, 695–707.

Dickinson, W.R., Beard, L.S., Brakenridge, G.R., Erjavec, J.L., Ferguson, R.C., Inman, K.F., Knepp, R.A., Lindberg, F.A., Ryberg, P.T., 1983. Provenance of north American Phanerozoic sandstones in relation to tectonic setting. Geological Society of America Bulletin 94, 222–235.

Doglioni, C., 1992. Main differences between thrust belts. Terra Nova 4, 152–164.

Doglioni, C., Fernandez, M., Gueguen, E., Sabat, F., 1999. On the interference between the early Apennines-Maghrebides back-arc extension and the Alps-Betics orogen in the Neogene geodynamics of the Western Mediterranean. Bollettino della Societa Geologica Italiana 118, 75–89.

Dou, Y., Yang, S., Liu, Z., Clift, P.D., Yu, H., Berne, S., Shi, X., 2010. Clay mineral evolution in the central Okinawa Trough since 28 ka: implications for sediment provenance and paleoenvironmental change. Palaeogeography, Palaeoclimatology, Palaeoecology 288, 108–117.

Drits, V.A., Sakharov, B.A., Lindgreen, H., Salyn, A., 1997. Sequential structure transformation of illite-smectite-vermiculite during diagenesis of Upper Jurassic shales from the North Sea and Denmark. Clay Minerals 32, 351–371.

Durand Delga, M., Rossi, P., Olivier, Ph., Puglisi, D., 2000. Situation et nature ophiolitique des roches basiques jurassiques associées aux flysch maghrébins du Rif (Maroc) et de Sicile (Italie). Comptes Rendus de l'Académie des Sciences, Paris 331, 29–38.

El Ouahabi, M., Daoudi, L., Fagel, N., 2014. Mineralogical and geotechnical characterization of clays from northern Morocco for their potential use in the ceramic industry. Clay Minerals 49, 35–51.

Eslinger, E., Mayer, L., Durst, T., Hower, J., Savin, S., 1973. A X-ray technique for distinguishing between detrital and secondary quartz in the fine grained fraction of sedimentary rocks. Journal of Sedimentary Petrology 43, 540–543.

Faleh, A., Sadiki, A., 2002. Glissement rotationnel de Dhar El Harrag: Exemplel'instabilité de terrain dans le Prérif central (Maroc). Bulletin de l'Institut Scientifique, Rabat 24, 41–48.

Folk, R.L., 1980. Petrology of Sedimentary Rocks. Hemphill's Austin (184 pp.).

Gibbs, R.J., 1977. Clay mineral segregation in the marine environment. Journal of Sedimentary Research 47, 237–243.

Guerrera, F., Martín-Martín, M., 2014. Geodynamic events reconstructed in the Betic, Maghrebian, and Apennine chains (central-western Tethys). Bulletin de la Société Géologique de France 185, 329–341.

Guerrera, F., Monaco, P., Nocchi, M., Parisi, G., Franchi, R., Vannucci, S., Giovannini, G., 1989. La Scaglia Variegata Eocenica nella sezione di Monte Cagnero (Bacino Marchigiano Interno): studio litostratigrafico, petrografico e biostratigrafico. Bollettino della Societa Geologica Italiana 107, 81–99.

Guerrera, F., Martin-Algarra, A., Perrone, V., 1993. Late Oligocene-Miocene syn-/-late-orogenic successions in Western and Central Mediterranean chains from the Betic Cordillera to the Southern Apennines. Terra Nova 5, 525–544.

Guerrera, F., Martín-Martín, M., Perrone, V., Tramontana, M., 2005. Tectono-sedimentary evolution of the southern branch of the Western Tethys (Magrebian Flysch Basin and Lucanian Ocean). Terra Nova 17, 358–367.

Guerrera, F., Estévez, A., López-Arcos, M., Martín-Martín, M., Martín-Pérez, J.A., Serrano, F., 2006. Paleogene tectono-sedimentary evolution of the Alicante Trough (External Betic Zone, SE Spain) and its bearing on the timing of the deformation of the South-Iberian Margin. Geodinamica Acta 19, 87–101.

Guerrera, F., Mancheño, M.A., Martín-Martín, M., Raffaelli, G., Rodríguez-Estrella Serrano, F., 2014. Paleogene evolution of the External Betic Zone and geodynamic implications. Geologica Acta 12, 171–192.

Guerrera, F., Martín-Martín, M., Raffaelli, G., Tramontana, M., 2015. The Early Miocene "Bisciaro volcaniclastic event" (northern Apennines, Italy): a key study for the geodynamic evolution of the central-western Mediterranean. International Journal of Earth Sciences (Geol Rundsch) 104, 1083–1106.

Guerrera, F., Martín-Martín, M., Tramontana, M., 2021. Evolutionary geological models of the central-western peri-Mediterranean chains: a review. International Geology Review 63, 65–86.

Henriquet, M., Dominguez, S., Barreca, G., Malavieille, J., Monaco, C., 2020. Structural and tectono-stratigraphic review of the Sicilian orogen and new insights from analogue modeling. Earth-Science Reviews, 103257 https://doi.org/10.1016/j.earscirev.2020.103257.

Holtzapffel, T., 1985. Les minéraux argileux: préparation, analyse diffractométrique et détermination. Société Géologique du Nord 12 (136 pp.).

Hunziker, J.C., 1986. The evolution of illite to muscovite: an example of the behavior of isotopes in low grade metamorphic terrains. Chemical Geology 57, 31–40.

Ingersoll, R.V., Bullard, T.F., Ford, R.L., Grimm, J.P., Pickle, J.D., Sares, S.W., 1984. The effect of grain size on detrital modes: a test of the Gazzi-Dickinson point-counting method. Journal of Sedimentary Research 54, 103–116.

Jabaloy-Sánchez, A., Azdimousa, A., Booth-Rea, G., Asebriy, L., Vázquez-Vílchez, M., Martínez-Martínez, J.M., Gabites, J., 2015. The structure of the Temsamane fold-and-thrust stack (eastern Rif, Morocco): evolution of a transpressional orogenic wedge. Tectonophysics 663, 150–176.

Khomsi, S., Bédir, M., Soussi, M., Ben Jemia, M.G., Ben Ismail-Lattrache, K., 2006. Highlight of middle-late Eocene compressional events in the subsurface of eastern Tunisia (Sahel): generality of the Atlasic phase in North Africa. Comptes Rendus Geoscience 338, 41–49.

Khomsi, S., Ben Jemia, M.G., de Frizon Lamotte, D., Maherssi, C., Echihi, O., Mezni, R., 2009. An overview of the late Cretaceous–Eocene positive inversions and oligo-Miocene subsidence events in the foreland of the Tunisian atlas: structural style and implications for the tectonic agenda of the Maghrebian atlas system. Tectonophysics 475, 38–582.

Lanson, B., Sakharov, B.A., Claret, F., Drits, V.A., 2009. Diagenetic smectite-to-illite transition in clay-rich sediments: a reappraisal of X-ray diffraction results using the multi-specimen method. American Journal of Science 309, 476–516.

Le Breton, E., Brune, S., Ustaszewski, K., Zahirovic, S., Seton, M., Müller, R.D., 2021. Kinematics and extent of the Piemont–Liguria Basin–implications for subduction processes in the Alps. Solid Earth 12, 885–913.

Lonergan, L., White, N., 1997. Origin of the Betic-Rif mountain belt. Tectonics 16, 504–522.

Lourens, L.J., Hilgen, F.J., Laskar, J., Shackleton, N.J., Wilson, D., 2004. The Neogene Period. In: Gradstein, F.M., Ogg, J.G., Smith, A.G. (Eds.), A Geologic Time Scale 2004. Cambridge University Press, pp. 409–440.

Maaté, S., Alcalá, F.J., Guerrera, F., Hlila, R., Maaté, A., Martín-Martín, M., Raffaelli, G., Serrano, F., Tramontana, M., 2017. The External Tanger Unit (Intrarifsub-Domain, External Rifian Zones, Morocco): an interdisciplinarystudy. Arabian Journal of Geosciences 10, 556. https://doi.org/10.1007/s12517-017-3347-8.

Maaté, S., Guerrera, F., Hlila, R., Maaté, A., Martín-Martín, M., Tramontana, M., 2018. New structural data on Tertiary of the External Tanger Unit (Intrarif, Morocco). Geogaceta 63, 123–126.

Martín-Algarra, A., 1987. Evolución geológica Alpina del contacto entre las Zonas Internas y las Zonas Externas de la Cordillera Bética. (Unplublished PhD Thesis)Universidad de Granada (1171 pp.).

Martini, E., 1971. Standard Tertiary and Quaternary calcareous nannoplankton zonation. In: Farinacci, A. (Ed.)Proceedings of the 2nd Planktonic Conference, Rome1970. Tecnoscienza, pp. 739–785.

Martín-Martín, M., Rey, J., Alcalá, F.J., Tosquella, J., Deramond, J., Lara-Corrona, E., Duranthon, F., Antoine, P.O., 2001. Tectonic controls on the deposits of a foreland basin: an example from the Eocene Corbières-Minervois basin, France. Basin Research 13, 419–433.

Martín-Martín, M., Guerrera, F., Hlila, R., Maaté, A., Maaté, S., Tramontana, M., Serrano, F., Cañaveras, J.C., Alcalá, F.J., Paton, D., 2022a. Tectono-sedimentary Cenozoic evolution of the El Habt and Ouezzane Tectonic units (External Rif, Morocco). Geosciences 18, 850–884.

Martín-Martín, M., Guerrera, F., Maaté, A., Hlila, R., Serrano, F., Cañaveras, J.C., Paton, D., Alcalá, F.J., Maaté, S., Tramontana, M., Martín-Pérez, J.A., 2022b. The Cenozoic evolution of the Intrarif (Rif, Morocco). Geosphere https://doi.org/10.1130/GES02199.1.

Martín-Ramos, J.D., Díaz-Hernández, J.L., Cambeses, A., Scarrow, J.H., López-Galindo, A., 2012. Pathways for quantitative analysis by X-ray diffraction. In: Aydinalp, C. (Ed.), An Introduction to the Study of Mineralogy. CumhurAydinalp, Intech Open, Tech, Rijeka, Croatia, pp. 73–92.

Michard, A., de Frizon Lamotte, D., Negro, F., 2007. Serpentinite slivers and metamorphism in the External Maghrebides: arguments for an intracontinental suture in the African paleomargin (Morocco, Algeria). Revista de la Sociedad Geológica de España 20, 173–185.

Michard, A., Mokhtari, A., Chalouan, A., Saddiqi, O., Rossi, Ph., Rjimati, E.-C., 2014. New ophiolite slivers in the External Rif belt, and tentative restoration of a dual Tethyan suture in the western Maghrebides. Bulletin de la Société Géologique de France 185, 313–328.

Michard, A., Mokhtari, A., Lach, Ph., Rossi, Ph., Chaouan, A., Saddiqi, O., Rjimati, E.-C., 2018. Liassic age of an oceanic gabbro of the External Rif (Morocco): implications for the Jurassic continent–ocean boundary of Northwest Africa. Comptes Rendus Geoscience 350, 299–309.

Moiroud, A., Martinez, M., Deconinck, J.F., Monna, F., Pellenard, P., Riquier, L., Company, M., 2012. High-resolution clay mineralogy as a proxy for orbital tuning: example of the Hauterivian-Barremian transition in the Betic Cordillera (SE Spain). Sedimentary Geology 282, 336–346.

Moore, D.M., Reynolds, R.C., 1997. X-Ray Diffraction and the Identification and Analysis of Clay Minerals. 2nd ed. Oxford University Press, Oxford, New York (378 pp.).

Müller, R.D., Zhirovic, S., Williams, S.E., Cannon, J., Seton, M., Bower, D.J., Tetley, M.G., Heine, C., Le Breton, E., Liu, S., 2018. A Global Plate Model including lithospheric deformation along major rifts and orogens since the Triassic. Tectonics 38, 1884–1907.

Müller, R.D., Zahirovic, S., Williams, S.E., Cannon, J., Seton, M., Bower, D.J., Tetley, M.G., Heine, C., Le Breton, E., Liu, S., Russel, S.H.J., Yang, T., Leonard, J., Gurnis, M., 2019. A Global Plate model including lithospheric deformation along major rifts and Orogens since the Triassic. Tectonics 38, 1884–1907. https://doi.org/10.1029/2018TC005462.

Nieto, E., Ortega-Huertas, M., Peacor, D.R., Aróstegui, J., 1996. Evolution of illite/smectite from early diagenesis through incipient metamorphism in sediments of the Basque-Cantabrian basin. Clays and Clay Minerals 44, 304–323.

Pantaloni, M., Picchezzi, R.M., D'Ambrogi, C., Pampaloni, M.L., Rossi, M., 2016. Note Illustrative della Carta Geologica d'Italia alla scala 1:50.000, foglio 280 Fossombrone. ISPRA, Servizio Geologico d'Italia 1–132.

Patchineelam, S.M., de Figueiredo, A.G., 2000. Preferential settling of smectite on the Amazon continental shelf. Geo-Marine Letters 20, 37–42.

Pletsch, T., 1997. Clay minerals in Cretaceous deep-water formations of the Rif and the Betic Cordillera. Bulletin Société Géologique du Nord 26, 1–106.

Rouvier, H., 1985. Géologie de l'Extrême Nord Tunisien: tectonique et paléogéographie superposées à l'extrémité orientale de la chaîne nord- maghrébine. Edition du Service géologique de Tunisie. Annales des mines et de la géologie 29 (427 pp.).

Serrano, F., 1992. Biostratigraphic control of Neogene volcanism in Sierra de Gata (south-east Spain). Geologie en Mijnbouw 71, 3–14.

Stampfli, G.M., Kozur, H.W., 2006. Europe from the Variscan to the Alpine Cycles. Geological Society of London 32, 5782.

Stampfli, G.M., Borel, G.D., Marchant, R., Mosar, J., 2002. Western Alps geological constraints on western Tethyan reconstructions. In: Rosenbaum, G., Lister, G.S. (Eds.), Reconstruction of the evolution of the Alpine-Himalayan orogen. Journal Virtual Explorer, pp. 77–106.

Suter, G., 1980a. Carte géologique du Rif, 1/500000. Notes et Mémoires du Service Géologique du Maroc, 245a.

Suter, G., 1980b. Carte structurale de la chaînerifaine à 1/500000. Notes et Mémoires du Service Géologique du Maroc, 245b.

Thiry, M., Jacquin, T., 1993. Clay mineral distribution related to rift activity, sea-level change and palaeoceanography in the cretaceous of the Atlantic Ocean. Clay Minerals 28, 61–84.
Tomassetti, L., Benedetti, A., Brandano, M., 2016. Middle Eocene seagrass facies from Apennine carbonate platforms (Italy). Sedimentary Geology 335, 136–149.
Tortosa, A., Palomares, M., Arribas, J., 1991. Quartz grain types in Holocene deposits from the Spanish Central System: some problems in provenance analysis. In: Morton, A.C., Todd, S.P., Haughton, P.D.W. (Eds.), Developments in Sedimentary Provenance Studies. Geological Society of London, Special Publicationsvol. 57, pp. 47–54.
Vázquez, M., Asebriy, L., Azdimousa, A., Jabaloy, A., Booth-Rea, G., Barbero, L., Mellini, M., González-Lodeiro, F., 2013. Evidence of extensional metamorphism associated to cretaceous rifting of the North- Maghrebian passive margin: the Tanger-Ketama unit (external Rif, northern Morocco). Geologica Acta 11, 277–293.
Vera, J.A., 2000. El Terciario de la Cordillera Bética: estado actual de conocimientos. Revista de la Sociedad Geológica de España 12, 345–373.
Vera, J.A., 2004. Geología de España. Sociedad Geologica de España; Instituto Geológico y Minero de España (884 pp.).
Vergés, J., Fernández, M., 2012. Tethys-Atlantic interaction along the Iberia-Africa plate boundary: the Betic-Rif orogenic system. Tectonophysics 579, 144–172.
Vissers, R.L.M., 2012. Extension in a convergent tectonic setting: a lithospheric view on the Alboran system of SW Europe. Géologie Belgique 15, 53–72.
Wade, B.S., Pearson, P.N., Berggren, W.A., Pälike, H., 2011. Review and revision of Cenozoic tropical planktonic foraminiferal biostratigraphy and calibration to the geomagnetic polarity and astronomical time scale. Earth-Science Reviews 104, 11–142.
Wildi, W., 1983. La chaˆne tello-rifaine (Algérie, Maroc, Tunisie): structure, stratigraphie et évolution du Trias au Miocène. Revue de Géographie Physique et de Géologie Dynamique 24, 201–297.
Zakir, A., Chalouan, A., Feinberg, H., 2004. Evolutiontectono-sédimentaire d'un domaine d'avant-chaîne : exemple des basin d'El-Habt et de Sidi Mrayt, Rif externe nord-occidental (Maroc) ; precisions stratigraphiques et modélisation tectonique. Bulletin de la Société Géologique de France 175, 383–397.
Zeck, H.P., 1996. Betic-Rif orogeny: subduction of Mesozoic Tethys lithosphere under eastward drifting Iberia, slab detachment shortly before 22 Ma, and subsequent uplift and extensional tectonics. Tectonophysics 254, 1–16.
Zuffa, G.G., 1980. Hybrid arenites: their composition and classification. Journal of Sedimentary Petrology 50, 21–29.
Zuffa, G.G., 1985. Optical analyses of arenites: Influence of methodology on compositional results. In: Zuffa, G.G. (Ed.), Provenance of Arenites. NATO ASI Series (Series C: Mathematical and Physical Sciences)vol. 148. Springer, Dordrecht, pp. 165–189.